INVESTIGATION OF COOLING EFFECT ON BiSrCaCuO SUPERCONDUCTOR BY USING SCANNING ELECTRON MICROSCOPY

by

NEVİN SOYLU

THESIS SUBMITTED TO

THE GRADUATE SCHOOL OF NATURAL AND APPLIED SCIENCES

OF

THE ABANT İZZET BAYSAL UNIVERSITY

IN PARTIAL FULFILLMENT OF THE REQUIREMENTS FOR THE DEGREE

OF

MASTER OF SCIENCE

IN THE DEPARTMENT OF PHYSICS

JUNE 2010

ABSTRACT

INVESTIGATION OF COOLING EFFECT ON BiSrCaCuO SUPERCONDUCTOR BY USING SCANNING ELECTRON MICROSCOPY

Soylu, Nevin
Master of Science , Department of Physics
Supervisor: Prof. Dr. Ahmet VARİLCİ

June 2010, 99 pages

In this thesis the effect of different cooling rate effects on BSCCO superconductors was investigated. For this sample after annealing at different speeds were cooled to room temperature. According to this cooling rate of temperature drop speed of 273 ° C / min, 136°C/ min, 55°C/ min, 25°C/min, 18°C/ min, respectively. Besides furnace cooling (5 ° C / min) and fast cooling process was also done.

Temperature resistivity measurements were made with 10 mA current , between 70 K-160 K temperature . In liquid nitrogen, the critical current density was calculated by measuring the critical current. SEM images were obtained to investigate the surface structure. BSCCO samples, the characteristic peaks of Bi-2212 and Bi-2223 was shown by X-ray measurements and Bi-2212 and Bi-2223 ratio was calculated.

136 ° C / min cooling rate and structure of specimens in the SEM image of the flake to be seen more, and this is more compatible of the critical temperature was observed. For Bi-2223 structure 273 ° C / min, 136 ° C / min cooling rate was found to be most suitable. Critical current density is highest at 5 ° C / min which is the slow rate of cooling and the critical current density of samples was found to be increased while the cooling speed is decreased .

Key Words: Superconductivity, BSCCO System, Cooling Rate, SEM, Critical Temperature, Critical Current Density

ÖZET

DEĞİŞİK SOĞUTMA ORANLARININ, ELEKTRON MİKROSKOBU KULLANARAK BiSrCaCuO SÜPERİLETKEN MALZEME ÜZERİNDEKİ ETKİSİNİN ARAŞTIRILMASI

Soylu, Nevin
Yüksek Lisans, Fizik Bölümü
Tez Danışmanı: Prof.Dr. Ahmet VARİLCİ

Haziran 2010, 99 sayfa

Farklı soğutma oranlarının BSCCO süperiletkenleri üzerindeki etkisi araştırıldı. Bunun için numuneler tavlama işlemlerinden sonra farklı hızlarda oda sıcaklığına soğutuldu. Bu soğutma oranlarına göre sıcaklık düşüş hızları 273°C/dk , 136°C/dk ,55°C/dk, 25°C/dk, 18°C/dk, olarak hesaplandı. Bunların yanında fırın soğutma (5°C/dk) ve hızlı soğutma işlemleri de yapıldı.

10 mA lik akım altında 70 K- 160 K sıcaklıkları arasında özdirenç ölçümleri yapıldı. Sıvı nitrojen içinde kritik akımları ölçülerek kritik akım yoğunlukları hesaplandı. Yüzey yapılarını araştırmak için SEM görüntüleri alındı. BSCCO örneklerinin Bi-2212 ve Bi-2223 karakteristik pikleri X-Ray ölçümleri ile görüntülendi ve Bi-2212 ve Bi-2223 oranları hesaplandı.

136°C/dk soğutma oranı ile hazırlanan numunede SEM görüntülerinde flake yapının daha fazla olduğu ve bunun da kritik sıcaklık değerinin yüksekliği ile uyumlu olduğu gözlendi. Bi-2223 yapıları için 273°C/dk, 136°C/dk soğutma oranlarının en uygun olduğu saptandı. Kritik akım yoğunluğunun en yüksek olduğu 5°C/dk ile en yavaş soğuma oranına sahip numune olduğu bulundu ve soğuma hızları düştükçe kritik akım yoğunluğunun arttığı gözlendi.

Anahtar Kelimeler : Süperiletkenlik, BSCCO Sistemi, Soğutma Oranları, SEM, Kritik Sıcaklık, Kritik Akım Yoğunluğu .

To my family…

ACKKNOWLEDGEMENT

It is a great pleasure to thank many people who have contributed to the completion of this thesis through their knowledge, guidance, support and friendship. At the beginning I owe a great deal to my supervisor Prof. Dr. Ahmet VARİLCİ for his patience, support, guidance , encouragement , supervision throughout of this thesis.

I would express my gratitude to my Co- supervisor Assoc. Prof. Dr. Cabir TERZİOĞLU.

I am grateful to Assistant Professor Mustafa AKDOĞAN for his effort during the sample preparation and measurement; Research Assistant Gürcan YILDIRIM for his help, effort and support during the preparation of this thesis.

.

Finally in my personal side I would like to thank my parents for their continuous supports , patience and encouragement which made it possible for me to continue my study.

TABLE OF CONTENTS

LIST OF TABLES

LIST OF FIGURES

CHAPTER 1

INTRODUCTION

1.1 The Historical Development of Superconductivity

In 1911 Kamerling Onnes from University of Leiden realized that the resistance of a thin thread of mercury sample felt to very low value when the temperature on the sample was reduced below 4.2 K (the boiling point of liquid helium). He also studied on different metals depicted in Figure1.1. As can be seen from the figure, the resistances of gold and platinum wires drop steadily to a constant value depending on the purity of the specimens. On the other hand, for mercury when the temperature is decreased, a sudden drop is observed to a low value on resistance. He named the new phenomenon as superconductivity.

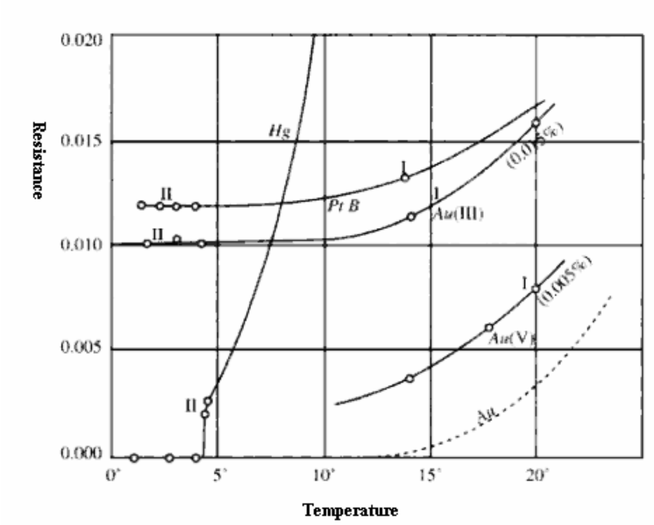

Figure 1.1- The resistance versus temperature graph for some metals

After all he chose the mercury an ideal metal to explain the superconductivity phenomenon was pure enough to show obviously the steady fall of resistivity to zero. In the years to follow it was discovered that many other metallic elements exhibit superconductivity at very low temperatures [1].

In 1933, one of the other surprising properties of the superconductivity was discovered by Meissner and Ochsenfeld: perfect diamagnetism. According to this theory; the magnetic flux is expelled from the interior of the superconductor sample when it is cooled below the critical temperature for superconductivity in weak external magnetic fields (Figure 1.2), which is called Meissner Effect [2].

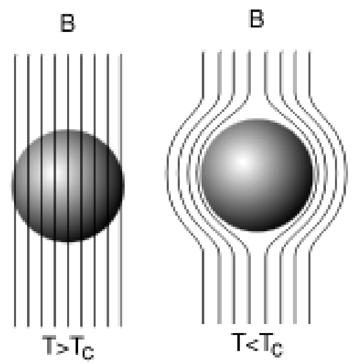

Figure 1.2- Expulsion of a weak external magnetic field from the interior of the superconducting material

Following the discovery of the Meissner Effect, F. and H. London [3] proposed a simple two–fluid model in 1934. The London model was functional enough either to explain Meissner effect or predict the penetration dept λ, a characteristic length of penetration of the static magnetic flux into superconductor.

In 1950 Vitaly Ginzburg and Lev Landau proposed an intuitive, phenomenological theory often called a macroscopic theory ' Ginzburg- Landau Theory ' of superconductivity [4] which replied to the characteristic properties of most interesting superconducting materials including high–T_c oxides. In 1957, Alexei Abrikosov also investigated the behavior superconductors in an external magnetic field and discovered that superconductor materials can be explained in two types: type-I and type-II superconductors [5]. While the former expels magnetic flux completely from their interior, the latter do it completely only at small fields, but partially in higher external fields. In 1957 John Bardeen, Leon Cooper and Robert Schrieffer proposed a complete microscopic theory of superconductivity that is usually referred to as the BCS Theory [6], of which the basis depends on the interaction of conduction electrons with elastic waves of the crystal lattice. Thus, not only does the BCS theory provide the basis for our present understanding of superconductivity in conventional materials but also some extent of the reference theory plays an important role in the on-going search for correct description of superconductivity in high–T_c cuprate oxides [7].

In 1962 Brian Josephson [8] postulated fascinating quantum tunneling effects that should occur when super current tunnels through an extremely thin layer roughly 10 Å of an insulator. The prediction was confirmed within a year and the effects are known as the Josephson effects. Superconducting technology based on these effects gradually evolved and in fact Josephson junction technology represents the basis of the promising superconducting electronics nowadays.

In that year, zero resistance and perfect diamagnetism were two main problems when properties of superconductivity were tried to use in the new technology. The former needs to get very low temperature for superconducting state. In these days, although people could supply this situation with using liquid helium but that was so expensive in those years. The latter is about the condition of disruption of superconductivity for any metal, when a magnetic field applied to, or current flowed through the sample so the practical value was decreasing in applications.

There would be a lot more practical uses for superconductivity unless it were for the very high cost of liquid helium coolant. Any gas will liquefy at sufficiently low temperatures; for example, oxygen becomes liquid at 90 K and nitrogen at 77 K. Moreover, it is far less costly to fluid these gases than to liquid helium. Liquid nitrogen has a much greater cooling capacity than liquid helium. For any application in which liquid nitrogen can replace liquid helium, the refrigeration cost will be about 1000 times less [9].

In 1973 powerful magnets were made with using Nb-Ti which is superconductor and in fact Nb_3Ge compound had the highest critical temperature, 23 Kelvin, in all superconductors. The high- temperature history of superconductivity started in late 1986 with J. George Bednorz and Karl Muller of the IBM research laboratory in Zurich, Switzerland [10]. They had reported the observation of superconductivity in lanthanum copper oxides doped with barium or strontium (La-Ba-Cu-O) at temperatures up to 38 K. Therefore the upper limit barrier is nearly 30 K for superconductivity that had been theoretically predicted almost 25 years earlier. This ceramic compound with perovskite structure was noted to be the first high temperature superconductor. Its multiphase nominal compound has the formula of $La_{5x}Ba_xCu_5O_{5(3-y)}$ whose critical temperature changes with regard to the change of x value. In $La_{2-x}Ba_xCuO_4$ compound the highest T_c value is obtained for x=0.15 [11]. Moreover, by using strontium instead of barium, the value of T_c can dramatically be increased up to about 36 K [12].

Hundreds of scientists rushed to try various chemical compounds to see which one would give the highest critical temperature. In February 1987 research groups in Alabama and Houston coordinated by K. Wu Ashburn and Paul Chu, discovered yttrium barium copper oxide ,Y-Ba-Cu-O, ceramics by using yttrium oxide instead of lanthanum oxide, with T_c=92 K [13]. This was an important discovery owing to the existence of a superconductor with a critical temperature above that of liquid nitrogen. It is very easy to prepare Y-Ba-Cu-O ceramics by mixing calcining and oxidizing the constituent powders (Figure1.3). The multiphase nominal compounds of this sample were noted to be $Y_{1.2}Ba_{0.3}Cu_2O_{4-x}$ and $Y_{0.6}Ba_{0.4}CuO_{3-x}$. Then scientists determined that the uniphase compound called as 1: 2: 3 or Y-Ba-Cu-O is $YBa_2Cu_3O_7$ by checking the ratios of barium yttrium and cooper. The difference between La-Ba-Cu-O and Y-Ba-Cu-O is pointed out to be oxygen vacancy. Depending on the vacancies, there is possibility of changing the critical temperature [14].

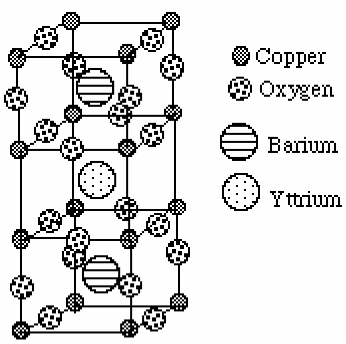

Figure1.3 - Unit cell for YBCO superconductor.

In 1987, a new chain is added to the superconductivity studies by Michael et al. who discovered the superconductivity bismuth strontium calcium copper oxide (Bi-Sr-Cu-O) ceramics [15]. In 1988, Maeda and his group observed superconductivity at 105 K by adding calcium to this system as Bi-Sr-Ca-Cu-O [16]. Also Tokano and his group found a stable superconductor at 110 K by adding lead to the compound [17]. In 1992 Quidwai and his group carried out the transition at 130-140 K by adding antimony to the system [18].

In 1988, Sheng and Parking observed superconductivity in thallium barium calcium copper oxide (Tl-Ba-Ca-Cu-O) compound at 110 K and 125 K. Nevertheless this compound either has carcinogenic effect or was unstable thus has to be produced each time. During these passing years, studies on different samples went on. In 1993 Schilling and his group observed superconductivity in mercury barium calcium copper oxide $HgBa_2CaCu_3O_{1+x}$ compound at 133 K; similarly, Chu and his group observed superconductivity in high pressure with Hg based compounds at 150 K [19], [20].

In 2001, J. Nagamatsu, J. Akimitsu and their group observed superconductivity in MgB_2 compound at 39 K, which was a very important discovery because of the fact that this critical temperature was quite high for Type-I superconductors [21] and elastic material so it had the advantage of being easy to be adapted to technology.

Table 1.1 High Critical Temperature Superconducting Compounds

Name	Formula[a]	Transition Temperature
Yttrium barium copper oxide	$Y_1Ba_2Cu_3O_7$	92 K
Bismuth strontium calcium copper oxide (2223 phase)	$(Bi,Pb)_2Sr_2Ca_2Cu_3O_x$	105
Thallium barium calcium copper oxide (1223 phase)	$Tl_1Ba_2Ca_2Cu_3O_y$	115
Mercury barium calcium copper oxide (1223 phase)	$Hg_1Ba_2Ca_2Cu_3O_y$	135[b]

[a]The subscripts (2223, etc.) provide a shorthand code for naming each generic compound
[b]Under extremely high pressure, $T_c > 150$ K has been observed.

In 2008, the discovery of a new family of high critical temperature iron and arsenic superconductors (AsFe) marked a second major revolution in the world of superconductivity. The new compounds, which do not contain copper (Cu) but which have oxygen (O), flour (F) or arsenic (As) and iron (Fe), will help scientists to solve some of the mysteries in the area of solid state physics and to answer some questions such as “Is the AsFe superconductor family really so different from second type superconductor?”. This point is fundamental to define a unified approach to the two families of superconducting materials.

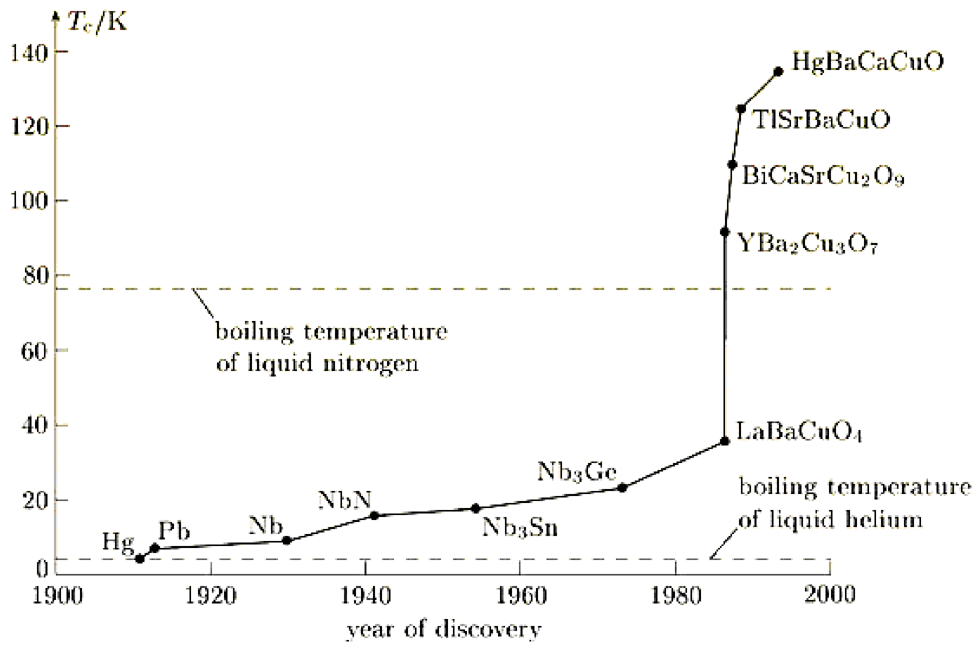

Figure 1.4- The critical temperature T_c of various superconductors plotted against their discovery date.

CHAPTER 2

THE PHYSICAL PROPERTIES OF SUPERCONDUCTIVITY

2. 1 Introduction

Provided that a material has to have the unique properties such as zero resistance to direct current; extremely high current carrying density; extremely low resistance at high frequencies; extremely low signal dispersion; high sensitivity to magnetic field; exclusion of externally applied magnetic field; rapid single flux quantum transfer; close to speed of light signal transmission, this material can be called as superconductor. Moreover, the most important of these basis properties are that; zero resistivity which means infinite conductivity under its critical temperature and the magnetic inductance which becomes zero inside the superconductor, when cooled below critical temperature in a weak external magnetic field.

2.2 Electrical Resistivity

How can a metal have infinite conductivity?

In fact, the electrical resistivity of all metals and alloys decreases when they are cooled. So firstly we have to think what causes a conductor to have resistance. A metal consists of a lattice of atoms , each with a shell of electrons. This can also be known as a positive ionic lattice. A normal metal consist of a regular crystalline lattice of positively charged ions and gas of free, on –interacting conduction electrons that fill the inter ionic space of lattice. If there is one electron per ion, we should have approximately $10^{23} electrons / cm^3$ .Because of the electrons are the opposite charge from the ions, the total charge is balanced and metal is electrically neutral. When an electrical potential difference is applied across the metal, the electrons drift from one end of the conductor to the other under the influence of the electrical field. Because of the external force accelerate the free electrons a current flow occurs within the metal.

So the current in a conductor is carried by "conduction electrons" which are free to move through the material. An electron is able to pass through a perfect crystal without any loss of momentum in its original direction . However, any fault in the periodicity of the crystal will scatter the electron and introduce some resistance. So there are two effects which can spoil the perfect periodicity of crystal lattice and so introduce resistance.

1. At temperatures above absolute zero the atoms are vibrating and electrons equilibrium positions will be displaced by various amounts. As we increase the temperature, the electrons also get scattered by thermal vibrations of the lattice, called phonons, so the resistivity rises with temperature. This contribution is called phonon resistivity, $\rho_P(T)$. When the temperature is lowered, the thermal vibrations of atoms decreases and the conduction electrons are less frequently scattered.

   A phonon, is a quantum of energy, relating to a mode of vibration occurring in a rigid crystal lattice, such as the atomic lattice of a solid.

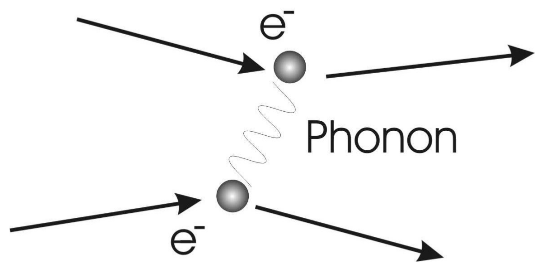

Figure 2.1- The schematic diagram of phonon resistivity

2. Foreign atoms or other defects (imperfections in periodicity like dislocations) randomly distributed can interrupt the perfect periodicity. As every real metal contains some imperfections and impurities, observes some finite resistivity at very low temperatures (extrapolated T=0) . Therefore the electrons, in addition to being scattered bye the impurities ,and this impurity scattering is more or less independent of temperature. As a result there is certain resistivity called "residual resistivity", ρ_i, which remains even at the lowest temperatures. The more impure the metal, the larger will be its residual resistivity. (Figure 2.2)

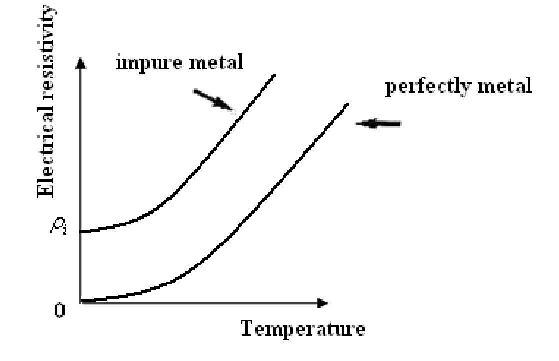

Figure 2.2- Variation of resistance of metals with temperature

Both thermal vibrations and any impurities or imperfections scatter the moving conduction electrons and give rise to electrical resistance.

$$\rho(T) = \rho_i + \rho_P(T) \qquad (2.1)$$

Near room temperatures, the thermal motion of ions is the primary source of scattering of electrons (due to destructive interference of free electron waves on non-correlating potentials of ions), and is thus the prime cause of metal resistance. Imperfections of lattice also contribute into resistance, although their contribution in pure metals is negligible.

The larger the cross-sectional areas of the conductor, the more electrons are available to carry the current, so the lower the resistance. The longer the conductor, the more scattering events occur in each electron's path through the material, so the higher the resistance.

And, some metals ,however, show a very remarkable behavior; when they are cooled their electrical resistance decrease in the usual way, but on reaching a temperature a few degrees above absolute zero they suddenly lose all trace of electrical resistance (Figure 2.3) . They are then said to have passed into the superconducting state. And this transformation to the superconducting state may occur even if the metal is so impure that it would otherwise have had large residual resistivity. [22]

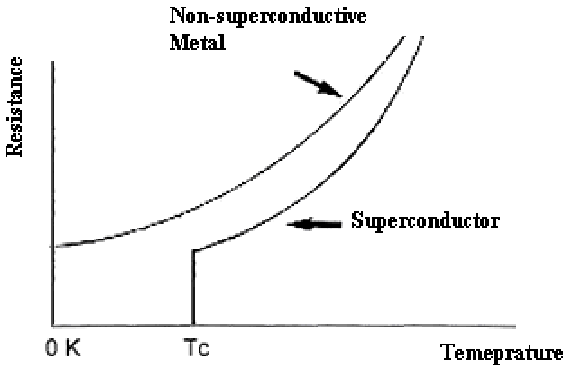

Figure 2.3 The difference of behavior ,non-superconductive metal and superconductor metal about loss of resistance at low temperatures.

2.3 Superconducting Transition Temperature

The temperature at which a superconductor loss electrical resistance is called its superconducting "transition temperature" or "critical temperature" and written as T_c, is different for each metal (Table 2.1). The transition is so sudden and complete that appears to different phase of matter. Above a critical temperature T_c the properties of metal are completely normal; below T_c superconducting properties are displayed, the most dramatic of which is the absence of any measurable DC electrical resistance[23].

In general the transition temperature is not very sensitive to small amounts of impurity, but the superconductivity of a few metals, such as iridium and molybdenum, which in the pure state have very low transition temperature, may be destroyed by presence of minute quantities of magnetic impurities. Such elements, therefore, only exhibit superconductivity if they are extremely pure, and specimens of these metals of normal commercial purity are not superconductors. Not all pure metals have been found to be superconductors; for example copper, iron and sodium have not shown superconductivity down to the lowest temperature to which they have so far been cooled.

Table 2.1 Values of Tc and Hc for the superconducting elements

ELEMENT		Tc (K)	Hc (GAUSS)
Al		1.196	99
Cd		0.56	30
Ga		1.091	51
Hf		0.09	—
Hg	α (rhomb)	4.15	411
	β	3.95	339
In		3.40	293
Ir		0.14	19
La	α (hcp)	4.9	798
	β (fcc)	6.06	1096
Mo		0.92	98
Nb		9.26	1980
Os		0.655	65
Pa		1.4	—
Pb		7.19	803
Re		1.698	198
Ru		0.49	66
Sn		3.72	305
Ta		4.48	830
Tc		7.77	1410
Th		1.368	162
Ti		0.39	100
Tl		2.39	171
U	α	0.68	—
	γ	1.80	—
V		5.30	1020
W		0.012	1
Zn		0.875	53
Zr		0.65	47

Superconductivity is not a rare phenomenon; about half the metallic elements are known to be superconductors and in addition a large number of alloys are superconductors. For an alloy it is possible to be a superconductor, even it is composed of two metals which are not themselves superconductors, such as Bi- Pd.

And in general some superconductor alloys have advantageous properties for applications about critical temperature. For example niobium is the metallic element with the highest transition temperature (9.3 K), but some alloys and metallic compounds remain superconducting up to even higher temperatures . For example Nb_3Sn has a transition temperature of about 18 K

Table 2.2 Superconducting Transition Temperatures of Some Alloys and Metalic Compounds Compared With Their Constituent Elements

	Nb	Pb	Ta	Sn	Zr
T_c(K	9.3	7.2	4.5	3.7	0.8

	Ta-Nb	Pb-Bi	Nb_3-Zr	Nb_3Sn	Nb_3Ge
T_c(K)	6.3	8	11	18	23

The eventuation of transition temperature of superconductors may be shown differences if the sample is pure or not. The transition to the superconducting state may be extremely sharp if the specimen is pure and physically perfect on cooling. For example in a good gallium specimen, the transition has been observed to occur within a temperature range 10^{-5} degrees. Adversely, if the specimen is impure or has a disturbed crystal structure the transition may be considerably broadened [22].

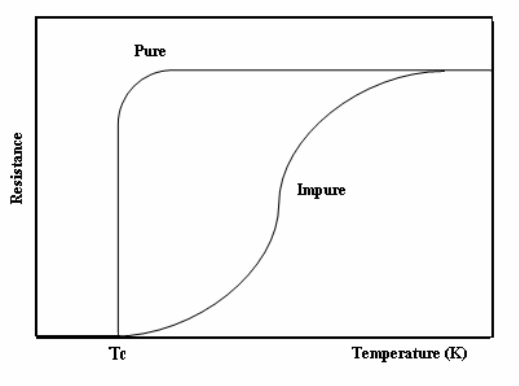

Figure 2.4 -The transition temperature for pure and impure superconductor metals

Table 2.3 Superconducting Elements

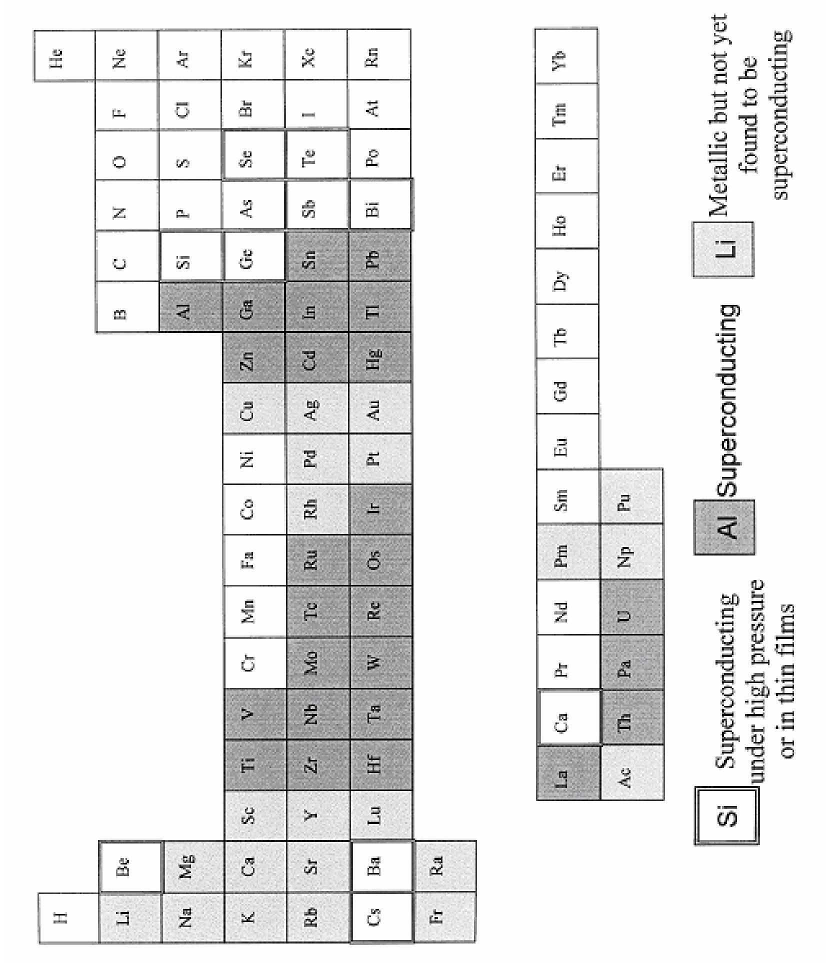

2.4 Zero Resistance

How can occur zero resistance and what is the reason of these phenomena?

Superconductivity was not sufficiently explained until 1957 when John Bardeen and his graduate assistants Leon Cooper and John Schrieffer proposed a microscopic explanation that would later be their namesake: the BCS Theory. This theoretical explanation later earned them the Nobel prize [6].

The BCS Theory is, in its simplest form, actually contradictory to our crude macroscopic view expressed earlier. As discussed earlier, superconductivity arises because electrons do not interact destructively with atoms in the crystal lattice of the material. The BCS Theory says that electrons do actually interact with the atoms, but constructively.

Cooper realized that atomic lattice vibrations were directly responsible for unifying the entire current. They forced the electrons to pair up into teams that could pass all of the obstacles which caused resistance in the conductor. These teams of electrons are known as Cooper pairs. Cooper and his colleagues knew that electrons which normally repel one another must feel an overwhelming attraction in superconductors. The answer to this problem was found to be in phonons, packets of sound waves present in the lattice as it vibrates. Although this lattice vibration cannot be heard, its role as a moderator is indispensable.

According to the theory, as one negatively charged electron passes by positively charged ions in the lattice of the superconductor, the lattice distorts. This in turn causes phonons to be emitted which form a trough of positive charges around the electron.

Before the electron passes by and before the lattice springs back to its normal position, a second electron is drawn into the trough. It is through this process that two electrons, which should repel one another, link up. The forces exerted by the phonons overcome the electrons' natural repulsion. The electron pairs are coherent with one another as they pass through the conductor in unison. The electrons are screened by the phonons and are separated by some distance. When one of the electrons that make up a Cooper pair and passes close to an ion in the crystal lattice, the attraction between the negative electron and the positive ion cause a vibration to pass from ion to ion until the other electron of the pair absorbs the vibration. The net effect is that the electron has emitted a phonon and the other electron has absorbed the phonon. It is this exchange that keeps the Cooper pairs together. It is important to understand, however, that the pairs are constantly breaking and reforming. Because electrons are indistinguishable particles, it is easier to think of them as permanently paired. Figure illustrates how two electrons, called Cooper pairs, become locked together.

By pairing off two by two the electrons pass through the superconductor more smoothly. The electron may be thought of as a car racing down a highway. As it speeds along, the car cleaves the air in front of it. Trailing behind the car is a vacuum, a vacancy in the atmosphere quickly filled by inrushing air. A tailgating car would be drawn along with the returning air into this vacuum. The rear car is, effectively, attracted to the one in front. As the negatively charged electrons pass through the crystal lattice of a material they draw the surrounding positive ion cores toward them. As the distorted lattice returns to its normal state another electron passing nearby will be attracted to the positive lattice in much the same way that a tailgater is drawn forward by the leading car.

The BCS theory successfully shows that electrons can be attracted to one another through interactions with the crystalline lattice. This occurs despite the fact that electrons have the same charge. When the atoms of the lattice oscillate as positive and negative regions, the electron pair is alternatively pulled together and pushed apart without a collision. The electron pairing is favorable because it has the effect of putting the material into a lower energy state. When electrons are linked together in pairs, they move through the superconductor in an orderly fashion.

As long as the superconductor is cooled to very low temperatures, the Cooper pairs stay intact, due to the reduced molecular motion. As the superconductor gains heat energy the vibrations in the lattice become more violent and break the pairs. As they break, superconductivity diminishes. This explains (roughly) why superconductivity requires low temperatures- the thermal vibration

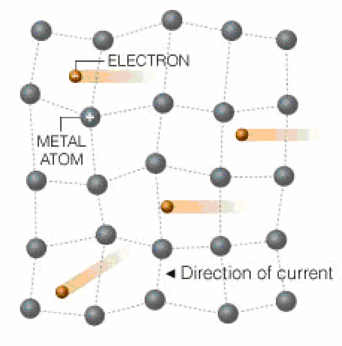

a) Electrons carrying an electrical current through a metal wire typically encounter resistance, which is caused by collisions and scattering as the particles move through the vibrating lattice of metal atoms and electrical resistance occurs.

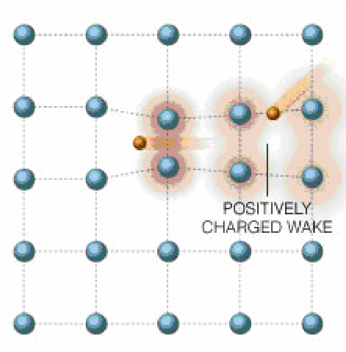

b) As the metal is cooled to low temperatures, the lattice vibration slows. A moving electron attracts nearby metal atoms, which create a positively charged wake behind the electron. This wake can attract another nearby electron

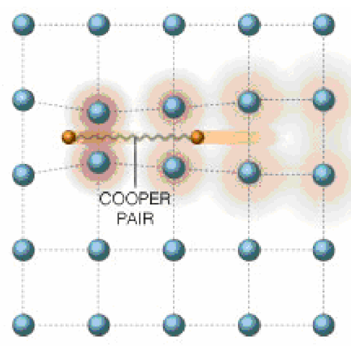

c) The two electrons form weak bond, called a Cooper pair, which encounters less resistance than two electrons moving separately. When more Cooper pairs form, they behave in the same way.

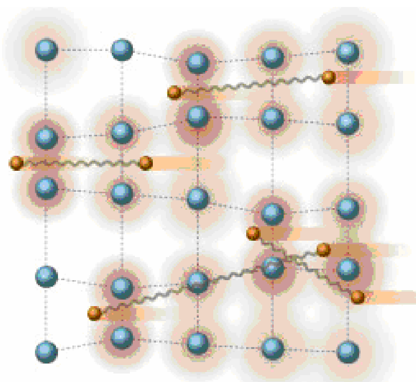

d) If a pair is scattered by an impurity, it will quickly get back in step with other pairs. This allows the electrons to flow un disturb through the lattice of metal atoms. With no resistance, the current may persist for years.

Figure 2.5- Occurrence of cooper pairs and their motion in the lattice

of the lattice must be small enough to allow the forming of Cooper pairs. In a superconductor, the current is made up of these Cooper pairs, rather than individual electrons, Figure(2.4) [24].

This BCS theory prediction of Cooper pair interaction with the crystal lattice has been verified experimentally by the isotope effect. That is, the critical temperature of a material depends on the mass of the nucleus of the atoms. If an isotope is used (neutrons are added to make it more massive), the critical temperature decreases. This effect is most evident in Type-I, and appears only weakly in Type-II.

This superconductivity of Cooper pairs is somewhat related to Bose-Einstein Condensation. The Cooper pairs act somewhat like bosons, which condense into their lowest energy level below the critical temperature, and lose electrical resistance [25].

The BCS Theory did exactly what a physical theory should do: it explained properties already witnessed in experiment, and it predicted experimentally verifiable phenomena. Though its specific quantitative elements were quite limited in their application (it only explained Type-I s-wave superconductivity), its essence was quite broad and has been modified applied to various other superconductors, such as Type-II perovskites.

Here the transition temperature T_c varies as $1/M^{1/2}$ where M is the mass of an isotope of a particular element. This pointed to the importance of lattice vibrations (whose frequency would be proportional to $M^{1/2}$) in mediating superconductivity [9].

In fact in the superconducting state the resistance falls to very small value, not zero. The resistance of any specimen may always be just less than the sensitivity of our apparatus allows us to detect. A more sensitive test, however, is to start a curret flowing round a closed superconducting ring and then see whether there is any decay in the current after a long period of time. Suppose the self inductance of the ring is L; then if at time t=0 we start a current i(0) flowing round the ring, at later time t the current will have decayed to

$$i(t) = i(0)\, e^{-(R/L)t} \qquad (2.2)$$

where R is the resistance of the ring. We can not measure the current into the circuit but can measure the magnetic field that the circulating current produces and see if the decays with time. The measurement of the magnetic field does not draw energy from the circuit, and we should be able to observe whether the current circulates indefinitely (Equation 2.2).

As can bee seen from equation for the smaller the inductance L of the circuit the more rapid the decay of current for a given value of resistance R and the more sensitive experiment[22].

2.5 Special Magnetic Behavior of A Superconductor

2.5.1 The Meissner Effect

The Meissner effect is the expulsion of a magnetic field from within a superconductor. This expulsion is different from merely not letting in an external field; any metal with infinite conductivity would do the latter. And this is not a consequence of infinite conductivity, but of another intrinsic characteristic property of the superconducting state. If it were so, then a superconductor cooled in the magnetic field through T_c , and the application of the magnetic field induces resistanceless currents which circulate on the surface of the specimen in such a manner as to create a magnetic flux density which everywhere inside the metal is exactly equal and opposite to the flux density of the applied magnetic field. And the net flux density inside the material remains at zero. This can be strengthened by a few elementary formula of electrodynamics.

Ohm' s law,

$$V = RI \tag{2.3}$$

and

$$E = \rho J \tag{2.4}$$

E , represents the electric field, ρ the resistivity and J the electrical current density in the sample. Zero resistivity implies zero electric field. So the Maxwell equation

$$curlE = -\frac{\partial B}{\partial t} \tag{2.5}$$

we have

$$\frac{\partial B}{\partial t} = 0 \tag{2.6}$$

This means that the magnetic field throughout the material must remain constant, the consequences of which are shown in Figure 2.5.

It is important to recognize that the exclusion of the magnetic field from inside a superconductor cannot be predicted by applying Maxwell's equations to a material at zero electrical resistance. We shall not only refer to a material that has zero resistance but does not exhibit the Meissner effect as a perfect conductor, but also show that a superconductor has additional properties besides those that can be predicted from its zero resistance [26].

The exclusion of the magnetic field from a superconductor takes place regardless of whether the sample becomes superconducting before or after the external magnetic field is applied. In the steady state, the external magnetic field is cancelled in the interior of the superconductor by opposing magnetic fields produced by a steady screening current flowing on the surface of the superconductor (Figure 2.6).

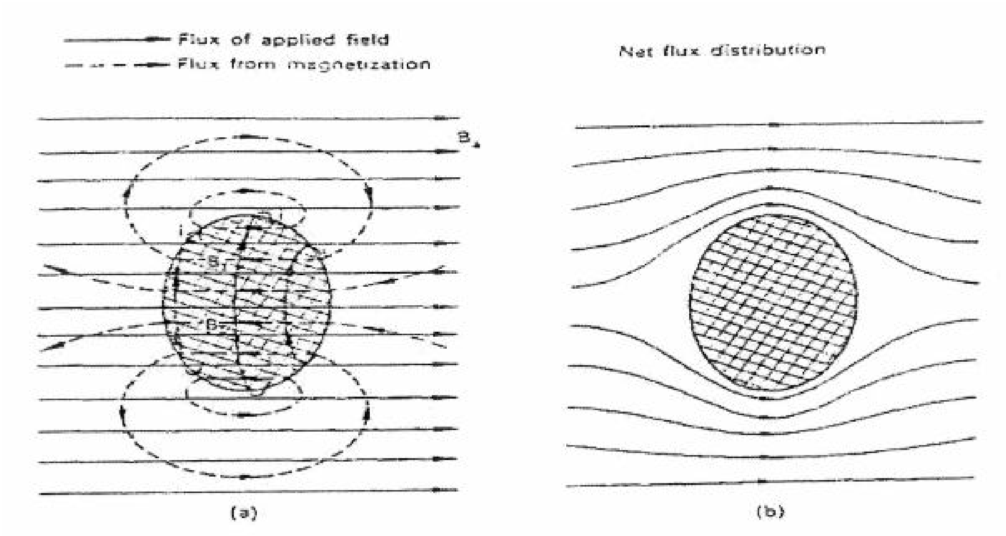

Figure 2.6 Distribution of magnetic flux about a perfectly diamagnetic body

In Figure 2.7 part (a) of this figure, a perfect conductor is cooled in zero magnetic field to below the temperature at which its resistance becomes zero. When a magnetic field is applied, screening currents are induced in the surface to maintain the field at zero within the material, and when the field is removed, the field within the material stays at zero. In contrast, part (b) shows that cooling of a perfect conductor to below its critical temperature in a uniform magnetic field leads to a situation where the uniform field is maintained within the material. Providing that the applied field is then removed, the field within the conductor remains uniform, and continuity of magnetic field lines means there is a field in the region around the perfect conductor. Clearly, the magnetization state of the perfect conductor depends not just on temperature and magnetic field, but on the previous history of the material as well.

Contrast this with the behavior of a superconductor, shown in Figure 2.6. Whether a material is cooled below its superconducting critical temperature in zero field (c), or in a finite field (d), the magnetic field within a superconducting material is always zero. The magnetic field is always expelled

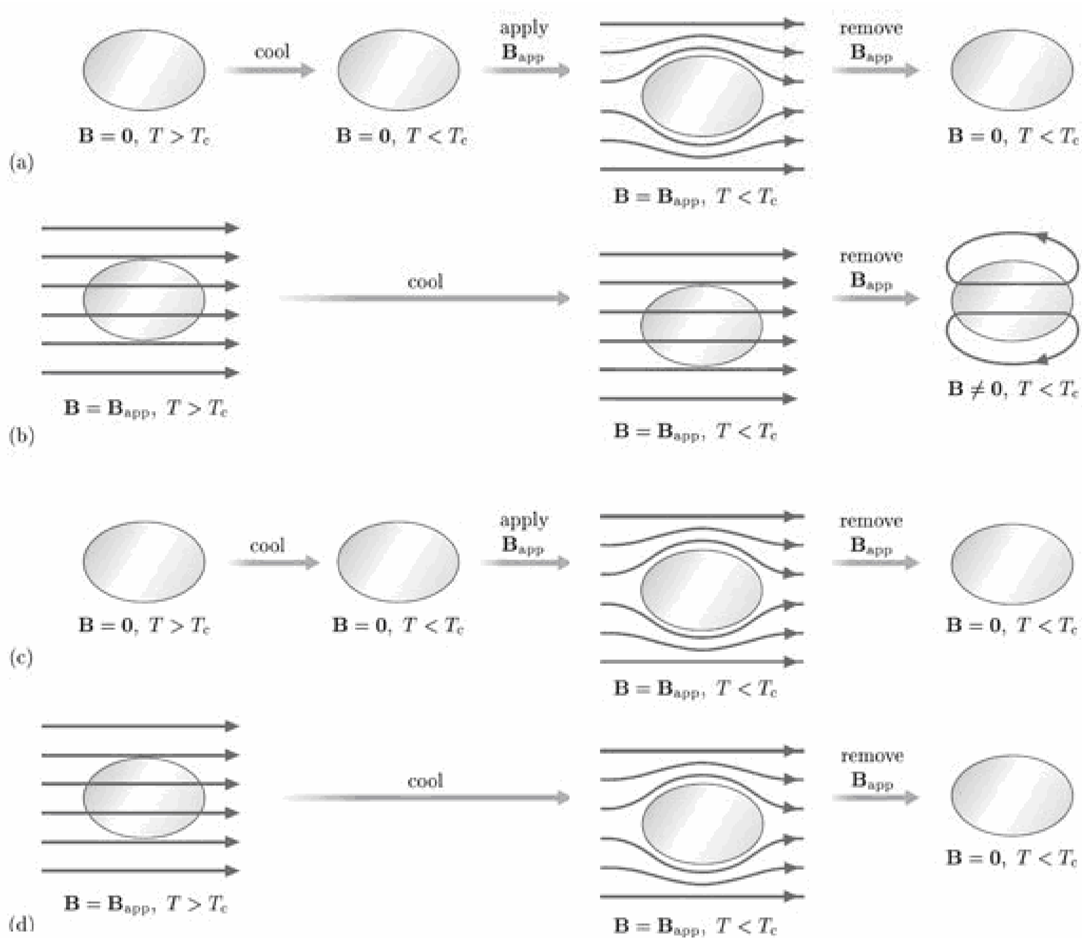

Figure 2.7 Magnetic behavior of a superconductor and a perfect diamagnetic specimen (a)-(c) Magnetic field applied after the specimen cooled below Tc. (b)-(d) Magnetic field applied before the specimen cooled below Tc.

from a superconductor, which is achieved spontaneously by producing currents on the surface of the superconductor. The direction of the currents is such as to create a magnetic field that exactly cancels the applied field in the superconductor. It is known as the Meissner effect, which distinguishes a superconductor from a perfect conductor at zero resistance. It is seen that the state of magnetization of a perfect conductor is not uniquely determined by the external conditions but depends on the sequence by which these conditions were arrived at [22]. Thus zero resistance and zero magnetic field can be regarded as the two key characteristics of superconductivity.

2.5.2 Perfect Diamagnetism

Diamagnetism is due to currents induced in atomic orbital by an applied magnetic field. The induced currents produce a magnetization within the diamagnetic material that opposes the applied field, and the magnetization disappears when the applied field is removed. However, this effect is very small: the magnetization generally reduces the applied field by less than one part in 10^5 within the material. In diamagnetic material, the magnetic field density $\mathbf{B} = \mu\mathbf{H}$, with the relative permeability μ slightly less than unity.

Superconductors take the diamagnetic effect to the extreme, since in a superconductor the field **B** is zero, which means that the field is completely screened from the interior of the material. Thus the relative permeability of a superconductor is zero.

2.5.3 Surface Currents

There are two types for surface currents. The first type is a 'reversible' or Meissner current which arises from the fact that if there is no pinning the equilibrium flux density in the material is slightly below the external value whether the field is increasing or decreasing.

The second one of surface current is caused by pinning of flux lines to the surface and is an irreversible effect, since the direction of the current depends on whether the field is increasing or decreasing. It usually produces a magnetization which is comparable with, but smaller than, the reversible magnetization [27].

As we know from the Meissner effect that a superconductor metal does not allow magnetic flux to exist in its interior, which has an important effect on electric currents that flow along the superconductor. The currents cannot pass through the body of the superconducting metal, but flow only on the surface. At any point in a material of unit permeability the relation between the magnetic flux and current density can be determined from Maxwell's equation.

$$\nabla \times B = \mu_0 J \tag{2.7}$$

As seen from the equation, provided that the metal is superconductor B is zero inside, and so curl B is must be zero inside. The current density J must also be zero within the superconductor.

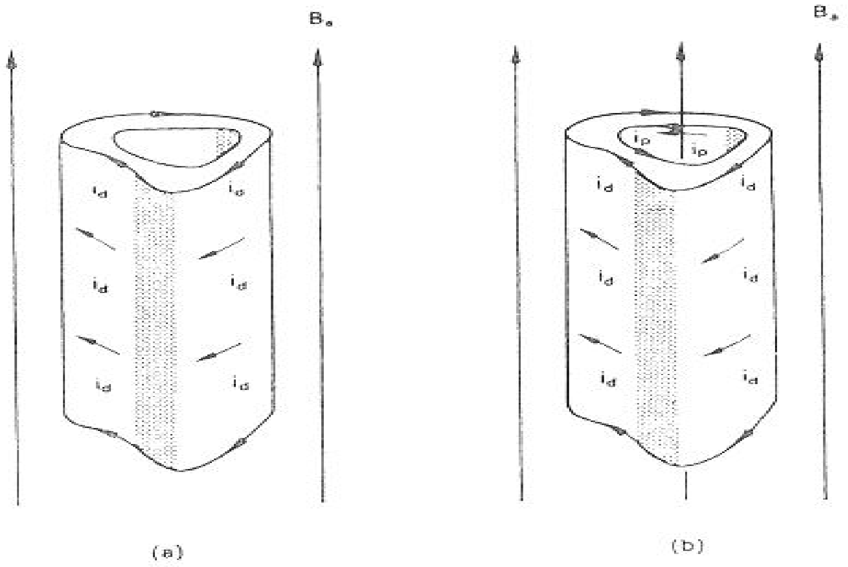

Figure 2.8 – Hollow superconductor. (a) Magnetic field applied when material is in the superconducting state. (b) Material become superconducting in an applied magnetic field

As shown from Figure 2.7, we shall consider the properties of a superconducting body with a hole right through it.

Firstly, suppose that the body (a) is cooled below its transition temperature. After it becomes superconductor, a magnetic field B_a is applied. The body is perfectly diamagnetic so there will be no flux density in the body. The perfect diamagnetism of the superconducting material is maintained bye currents $\boldsymbol{i_d}$ which circulate on the outer surface so as the cancel the flux in the metal. However, the flux density generated by these diamagnetic screening currents also cancel the flux density due to the applied field in the hole. In this situation the superconducting body is not different from merely resistanceless body. The current induced on the outer surface bye the application of the magnetic field cansels the flux inside.

Now consider a situation in which a superconductor behaves differently from a merely resistanceless body, or “perfect” conductor. Suppose the magnetic field is applied before the body is cooled below its transition temperature. Above Tc the magnetic flux passes both through the body and the hole. If the sample were a perfect conductor this flux distribution will not change when the body would lose its resistance, and no currents would appear on the surface. A superconductor, however ,behaves differently; below Tc the material becomes perfectly diamagnetic but though there is no flux though the material , flux remains in the hole (b). Currents must circulate to maintain these differences in the flux density. Diamagnetic surface currents i_d which cancel the flux in the hole, so if there is magnetic flux threading the hole this must be generated by currents i_p circulating in the opposite (paramagnetic) direction around its periphery. We have, therefore, the result that flux threading a hole or normal region through a superconductor is always associated with a current circulating around the boundary.

The net circulating current i_p- i_d is that generates a flux density equal to the difference between the flux density in the hole and outside the superconducting body [22].

2.5.4 The London Theory

The Meissner effect could not be explained by any conventional model of electricity in solids, but a bold hypothesis was put forth by F. and H. London. Since current flows unimpeded within a superconductor, let there be circulating currents inside the superconductor which set up a magnetic field that exactly cancels the magnetic field being applied externally. The form required for such a circulating current turns out to be surprisingly simple. The London equations deal with the electrodynamics behavior of superconductors on a macroscopic scale. They relate the local electric (**E**) and magnetic (**B**) fields to the super current density **J** . As we know the force can be written this,

$$F = m\frac{d}{dt}\left(v_s\right) \tag{2.8}$$

Here v_s is superelectron's velocity ,

$$J_s = n_s e v_s \tag{2.9}$$

$$F = qE \tag{2.10}$$

We combine these equations ;

$$eE = m\frac{d}{dt}\left(\frac{J_S}{n_s e}\right) \tag{2.11}$$

$$E = \frac{d}{dt}\left(\frac{m}{n_s e^2}J_S\right) \tag{2.12}$$

$$\frac{n_s e^2 E}{m} = \frac{dJ_S}{dt} \tag{2.13}$$

If we curl the two sides of the equation,

$$\vec{\nabla} \times \frac{n_s e^2 \vec{E}}{m} = \vec{\nabla} \times \frac{d\vec{J}_S}{dt} \tag{2.14}$$

Using Faraday's law to,

$$\nabla \times E = -\frac{dB}{dt} \tag{2.15}$$

Regulating the equation

$$-\frac{n_s e^2}{m} \frac{d\vec{B}}{dt} = \vec{\nabla} \times \frac{d\vec{J}_S}{dt} \tag{2.16}$$

We can obtain

$$\frac{d}{dt}\left[\vec{\nabla} \times \vec{J}_S + \frac{n_s e^2}{m} \vec{B}\right] = 0 \tag{2.17}$$

As we know B=0 inside a superconductor

$$\vec{\nabla} \times \vec{J}_S = -\frac{n_s e^2}{m} \vec{B} \tag{2.18}$$

For the result Faraday's law to and some mathematical operations;

$$\vec{\nabla} \times \vec{B} = \mu_0 J + \mu_0 \varepsilon_0 \frac{\partial \vec{E}}{\partial t} \tag{2.19}$$

$$\vec{\nabla} \times \vec{\nabla} \times \vec{B} = \mu_0 \vec{\nabla} \times J \tag{2.20}$$

$$\vec{\nabla}\left(\vec{\nabla} \cdot \vec{B}\right) - \vec{\nabla}^2 \vec{B} = -\mu_0 \frac{n_s e^2}{m} \vec{B} \tag{2.21}$$

The result is obtained.

$$\vec{\nabla}^2 \vec{B} = \mu_0 \frac{n_s e^2}{m} \vec{B} \tag{2.22}$$

To make shorter this ,

$$\lambda^2 = \frac{m}{\mu_0 n_s e^2} \tag{2.23}$$

And the main equation is reached

$$\vec{\nabla}^2 \vec{B} = \frac{1}{\lambda^2} \vec{B} \tag{2.24}$$

The only *constant* solution inside the superconductor must be **B** = 0, which is another way of saying that magnetic fields are excluded. The variable solution has the general form

$$B(x) = B_0 \exp(-x / \lambda_L) \tag{2.25}$$

The λ which on the equation 2.23 , the value is called the *London penetration depth*. The hypothesis of circulating shielding currents thus give a concise account of the Meissner effect; is all that is needed. Years later, when the BCS theory came along and justified the London equation, the issue was settled satisfactorily [9].

2.5.5 The Magnetic London Penetration Depth

Penetration Depth is a measure of how deep light or any electromagnetic radiation can penetrate into a material. It is defined as the depth at which the intensity of the radiation inside the material falls to 1/e (about 37%) of the original value at the surface.

As we know the perfect diamagnetism of a superconductor prevents electrical currents flowing through the body material. This cannot be true at the surface of the superconductor.

In fact the currents can not be confined entirely to the surface because, if this were so the current sheet would have no thickness and the current density would be infinite, which is physical impossibility. Actually the currents flow within a very thin surface layer whose thickness is of the order of 10^{-5} cm, although the exact value varies for different metals. The thickness is so small but it plays very important part in determining the properties of superconductors.

As we know screening currents circulating to cancel the flux inside must flow within the surface layer and so the flux density does not fall abruptly to zero at the boundary of the metal but dies away within the region where the screening currents are flowing. The depth of this region the flux of the applied magnetic field appears to penetrate, is called the "penetration depth" and is represented λ .

If at a distance x into the metal the flux density falls to a value B(x) ,we can define the penetration depth λ by

$$\int_0^\infty B(x)dx = \lambda B(0), \tag{2.26}$$

There is a predict, by London , that in a specimen which is much thicker than the penetration depth the magnetic flux density decays exponentially as it penetrates into the metal, i.e.

$$B(x) = B(0)e^{-x/\lambda} \tag{2.27}$$

B(0) is the flux density at the surface of the metal. This formulation gives us, there would be the same amount of flux inside the superconductor the flux density of the external field remained constant to distance λ into the metal.(Figure 2.9)

Using a approximation that the flux density B(0) of the applied field remains constant to a distance λ into the metal then abruptly to zero.

Because the penetration is so small we do not notice the flux penetration in magnetic measurements .

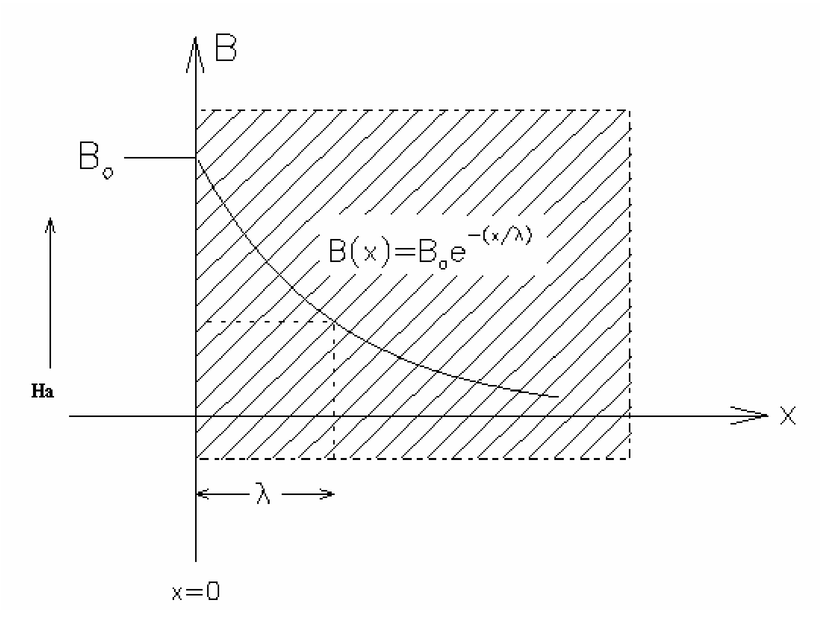

Figure 2.9 Variation of flux density at boundary of a superconductor.

The penetration depth does not have a fixed value but varies with temperature ,Figure 2.10

We can estimate a value for λ by assuming that all of the free electrons are superconducting. If we set $n_s = 10^{29}\ m^{-3}$, a typical free electron density in a metal, then we find that

$$\lambda = \left(\frac{m}{\mu_0 n_s e^2} \right)^{1/2} = 1.7 \times 10^{-8} m \cong 20nm \qquad (2.28)$$

penetration depth, depends on the number density n_s of superconducting electrons. The number density of superconducting electrons depends on temperature, so the penetration depth is temperature dependent. For $T << T_c$, all of the free electrons are superconducting, but the number density falls steadily with increasing temperature until it reaches zero at the critical temperature. Since $\lambda \propto n_s^{-1/2}$ according to the London model, the penetration depth increases as the temperature approaches the critical temperature, becoming effectively infinite – corresponding to a uniform field in the material – at and above the critical temperature. Figure 2.9 shows this temperature dependence for tin, which is well represented by the expression according the empirical expression;[28].

$$\lambda(T) = \frac{\lambda(0)}{\left[1-(T/T_c)^4\right]^{1/2}} \qquad (2.29)$$

where λ(0) is the value of the penetration depth at $T = 0$ K

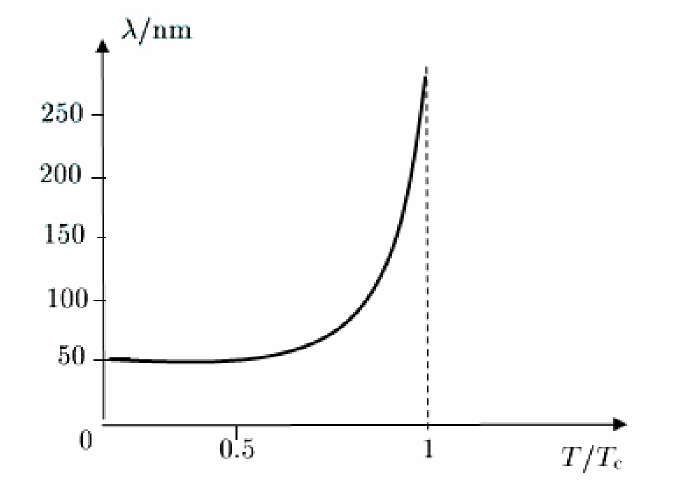

Figure 2.10 Variation of penetration depth with temperature

Perfect diamagnetism does not, therefore, occur in specimens, which are very close to their transition temperature. The decrease in penetration depth is, however, so rapid as the temperature falls below T_c that any large departure from perfect diamagnetism would be extremely difficult to detect in bulk specimens because of the difficulty of holding the temperature sufficiently constant during a measurement. For example, to observe a penetration depth of about 1 mm a specimen would, which is shown in above formula, have to be held at a temperature only 10^{-7} percent below the transition temperature.[22]

The penetration depth in a superconducting metal also depends on the purity, the penetration depth increasing as the metal becomes more impure. For example, in tin containing 3% indium the penetration depth is twice that pure tin.

2.5.6 The Coherence Length

The solution to the London equation showed that a magnetic field could penetrate a little way into a superconductor; equation (2.27) says that the field falls off exponentially over a mean distance λ_L known as the *penetration depth.* Typically this is less than $0.05\mu m$ and so a macroscopic sample of a superconductor could safely be said to entirely exclude magnetic fields. But what happens on a scale smaller than λ ?

A central contribution to the theory of superconductivity was made by Ginsburg and Landau, who introduced the notion of a *coherence length,* generally denoted by ξ . By the time of their hypothesis, superconductivity was agreed to be an interaction among electrons, and so it was natural to imagine this interaction occurring within some limited distance. Coherence length ξ, given by

$$\xi = \sqrt{\frac{\hbar^2}{2m|a|}} \tag{2.30}$$

which describes the size of thermodynamic fluctuations in the superconducting phase.

The ratio $\kappa = \lambda/\xi$ is known as the Ginsburg–Landau parameter. (We will explain in section 2.7 ,Type-I and type –II superconductors .)

Type-I superconductors are those with $0 < \kappa < 1/\sqrt{2}$, and Type-II superconductors those with $\kappa > 1/\sqrt{2}$ .For Type II superconductors, the phase transition from the normal state is of second order, for Type-I superconductors it is of first order. This is proved by deriving a *dual Ginzburg–Landau theory* for the superconductor[9].

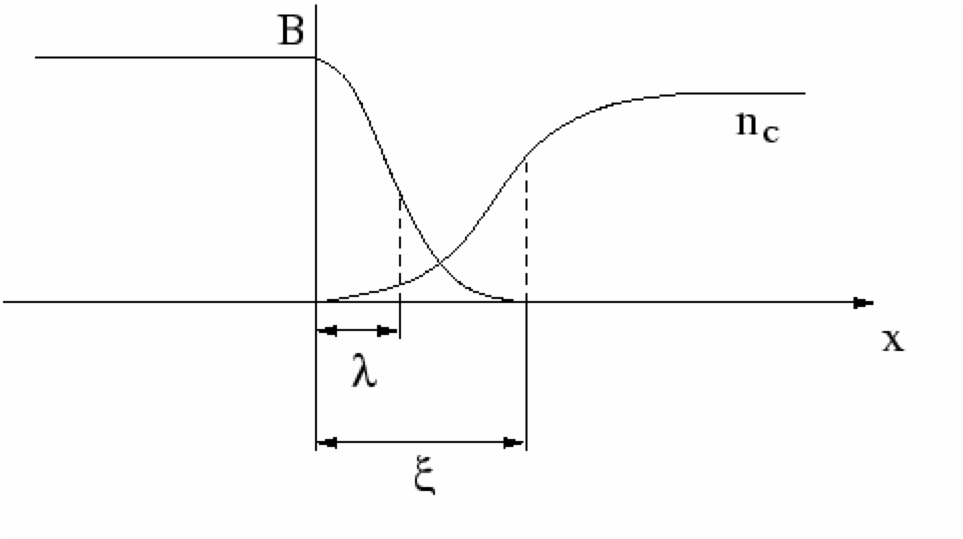

Figure 2.11 The penetration depth and coherence length in a superconductor metal.

Table 2.4 Penetration Depth and Coherence Length of Selected Superconductors at T=0K

Superconductor	**λ (nm)**	**ξ (nm)**
Al	16	160
Cd	110	760
Pb	37	**83**
Nb	39	**38**
Sn	34	**23**

2.5.7 The Critical Magnetic Field

The superconducting state cannot exist in the presence of a magnetic field greater than a critical value, even at absolute zero. This critical magnetic field is strongly correlated with the critical temperature for the superconductor, which is in turn correlated with the band gap. This is an important characteristic of a superconductor is that its normal resistance is restored if a sufficiently large magnetic field is applied.

If a metal is to remain superconducting, the net momentum of the super electrons must not exceed a certain value. For this reason there is a limit to the density of resistanceless current that can be carried by any region in the metal. Let us call this the "*critical current density*" J_c of the metal. This critical current affects to both a screening currents passed along the specimen from an external source and to screening currents which shield the specimen from an applied magnetic field. As a result of this critical current density , a superconducting metal will be driven normal if a sufficiently strong field is applied to it.

If the strength of the applied field is increased the shielding currents must also increase in order to maintain perfect diamagnetism. And critical current density will be reached by the shielding currents and the metal will lose its superconductivity. The shielding currents then cease and the flux due to the applied magnetic field is no longer cancelled within the metal. There is therefore a limit to the strength of magnetic field which can be applied to a superconductor if it is to remain superconducting.

We can say there is definite relationship between the supercurrent density and the magnetic flux density. The critical current density will therefore be reached at the surface when the flux density of the magnetic field is increased to a certain value. We may call this the "critical flux density" B_c or "critical magnetic field strength" H_c where

$$H_c = B_c / \mu_0 \qquad (2.31)$$

μ_0 permeability is of free space obtains in response to an applied magnetic field.

If the critical magnetic field of a superconductor is measured, its value is found to depend on the temperature. At very low temperatures, the critical field strength is essentially independent of temperature, but as the temperature increases, the critical field strength drops, and becomes zero at the critical temperature. At temperatures just below the critical temperature it requires only a very small magnetic field to destroy the superconductivity. (Figure 2.12)

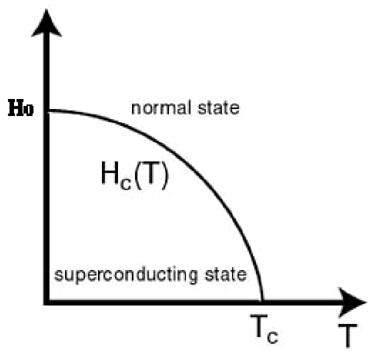

Figure 2.12. Phase diagram of a superconductor, showing variation with temperature of the critical magnetic field.

The temperature dependence of the critical field strength is approximately parabolic. It has merely been found experimentally that the variation can be conveniently described to within a few per cent by a parabolic curve. The experimental curves are not in fact exactly parabolas, and to describe them accurately one would need a polynomial expression [29].

$$H_c = H_0\left[1-\left(\frac{T}{T_c}\right)^2\right] \tag{2.32}$$

The value of H_0 is different for each superconducting metal; metals with low transition temperatures have low critical fields at absolute zero. So each superconductor has a different phase diagram ,Figure 2.13 .

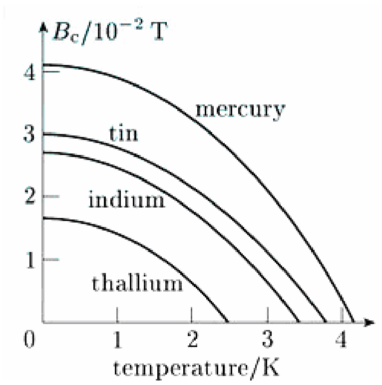

Figure 2.13. Critical fields of some superconductors.

2.6 Critical Currents

Since there is no loss in electrical energy when superconductors carry electrical current, relatively narrow wires made of superconducting materials can be used to carry huge currents. However, there is a certain maximum current that these materials can be made to carry, above which they stop being superconductors. If too much current is pushed through a superconductor, it will revert to the normal state even though it may be below its transition temperature.

As we show that the critical current is related to the critical magnetic field strength H_c. All currents in a superconductor flow at the surface within the penetration depth, the currents density decreasing rapidly from some value Ja at the surface .And superconductivity breaks down if the suppercurrent density exceeds a certain value which we call the critical current density Jc . As we know there can be two contributions to the current flowing on the surface of a superconductor. If a superconductor wire along which passing a current from some external source such as battery .We call this current the “transport current” because it transport charge into and out of the wire. If the wire is in an applied magnetic field screening currents are superimposed on the transport current, and at any point the current density J can be considered to the sum of a component J_i due to the transport current and a component J_H which arises from the screening currents

$$J= J_i+ J_H \qquad (2.33)$$

The value of Critical Current Density (J_c) is a function of temperature; i.e., the colder you keep the superconductor the more current it can carry as a result of Ohm’s Low , lower resistance higher current, as we know[22].

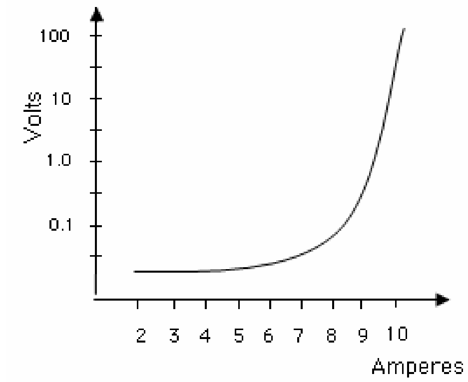

Figure 2.14.Current versus with voltage and critical temperature for superconductor metal.

As we know the critical magnetic field strength Hc depends on the temperature. As the temperature becomes higher , the critical current becomes smaller. The relation between the critical current and temperature is plotted with closed circles in Figure 2.15. It clearly shows that the critical temperature monotonically decrease with the temperature. A solid line in the figure is drawn on the basis of the Ginzburg-Landau (GL) theory, which states that the critical current is in proportion to $(1\text{-}T/T_c)^{3/2}$. T_c means the critical current and a coefficient is an adjustable parameter. The observed data agree well with the theory, when the coefficient is 225 mA.

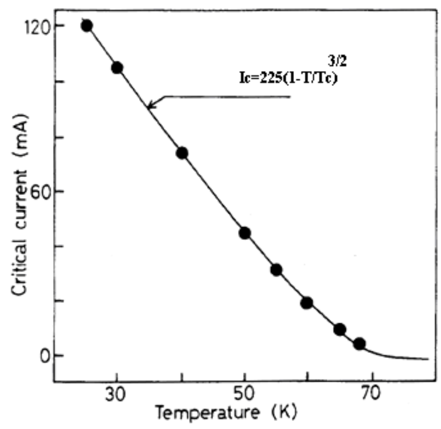

Figure 2.15. The temperature dependence of the critical current. Closed circles are obtained from the experiment. A solid line was drawn on the basis of the Ginzburg-Landau theory.

2.7 Type-I and Type–II Superconductors

Superconductive materials are divided into two part, type-I and type-II superconductors, also known as *soft* and *hard* superconductors, because of the dramatic difference in their magnetic and current-carrying properties. Pure or soft metals are generally shown type-I features, alloys and transition metals are shown type-II, characterized as the "hard" superconductors and there is no difference about the superconductivity mechanism.

The response to an applied magnetic field is quite different in the two cases. Meissner effect; for type –I superconductor there is exact cancellation of an applied magnetic field H by an equal and opposite magnetization M, resulting in magnetic field strength is zero inside the superconductor. Above the critical field, superconductivity vanishes. (In a perfect diamagnet M=-H, so that B=0 inside .)

In type-II superconductors, the Meissner effect is partially circumvented. The magnetic field starts penetrating into the material at a lower critical field H_{c1}. Penetration increases until at the upper critical field H_{c2} the material is fully penetrated and the normal state is restored. Figure 2-17 shows this behavior, in which M rises to a negative maximum at but then M retreats as flux lines begin to penetrate. The cancellation of H by M is no longer perfect, and B is finite within the superconducting material.

With the exception of V and Nb, all superconducting elements and most of their alloys in the dilute limit are type-I superconductors. The strength of the applied magnetic field required to completely destroy the perfect diamagnetism in the interior of the of the superconducting specimen is called the thermodynamic critical field strength Bc, as schematically as shown Figure 2.16. They exhibit a very sharp transition to a superconducting state and "perfect diamagnetism" - the ability to repel a magnetic field completely.

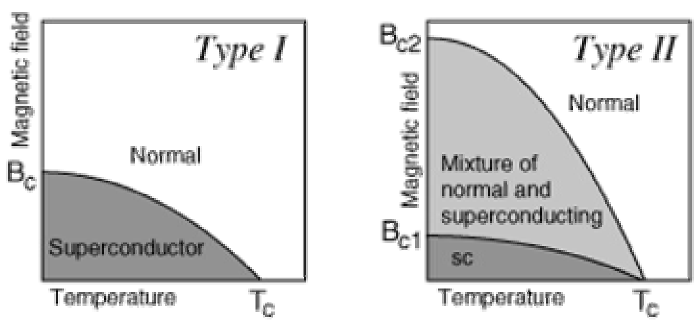

Figure 2.16. Critical magnetic field as a function of temperature for Type-I superconductors and Type-II superconductors.

In Type-II superconductors, the magnetic field can penetrate the sample in the form of quantized magnetic flux bundles, known as vortices.

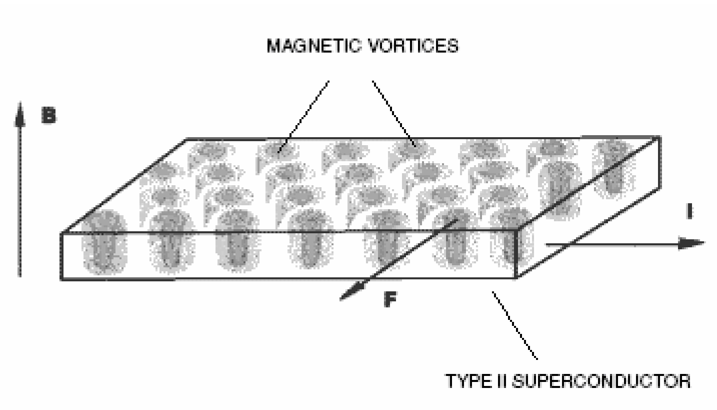

a)

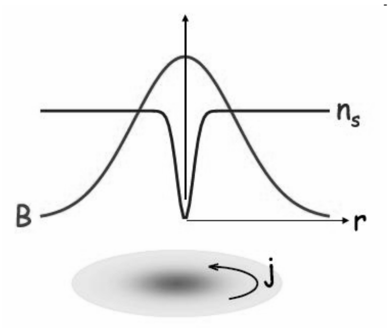

b)

Figure 2.17. a) Magnetic vortices in Type-II superconductors. b) Number density of superelectrons $n_{s(\mathrm{r})}$ and magnetic field strength B (r) around normal cores in the centre for one vortex tube a Type-II superconductor

A current density **j** flowing through the vortex lattice perpendicular to the magnetic field leads to a Lorentz force ($\mathbf{f}_L = \mathbf{j} \times \mathbf{B}$) on each vortex. This force tends to move the vortex liquid in the direction perpendicular to current and field. If the vortices start to flow into this direction, work is done and there is energy dissipation, the vortex motion directly leads to a finite resistance. In the mixed state, superconductors only have zero resistance when the vortices are pinned and unable to move [30].

For any superconductor, when a magnetic field is first applied to it, the Meissner effect will try to expel that field. As the field is increased, it costs more energy to expel it, and the free energy difference between normal and superconducting states diminishes. A Type –I superconductor always has a positive surface energy, so it expels a field as much as it can, until the normal and superconducting free energies are equal, beyond which point superconductivity vanishes.

By contrast, a Type-II superconductor expels a field for a while (up to H_{c1}), but as the applied magnetic field increases further the surface energy associated with the border becomes negative, so it is energetically favorable to let some of the material switch to the normal state in order to accommodate the flux lines of the field. Small circular regions form, which are normal inside but have superconducting currents circulating outside to shield the magnetic field—hence the name *vortex state.* The first penetration of flux lines occurs at H_{c-1}, where a single flux quantum Φ_0 occupies a core of approximate radius equal to the coherence length ξ. However, the spacing between them approximately equals the penetration depth .Thus the measured value of offers a way to estimate

$$\Phi_0 = H_{c1}\pi\lambda^2 \qquad (2.34)$$

In the same way, we can estimate the coherence length by examining the final state of the material just before it goes normal. At H_{c2} the vortex lattice and the pairing of the electrons disappear and the material becomes normal, the maximum number of flux lines have penetrated; there is no room for any more. The cores are packed tightly, only apart. This condition corresponds to: [9]

$$\Phi_0 = H_{c2}\pi\xi^2 \tag{2.35}$$

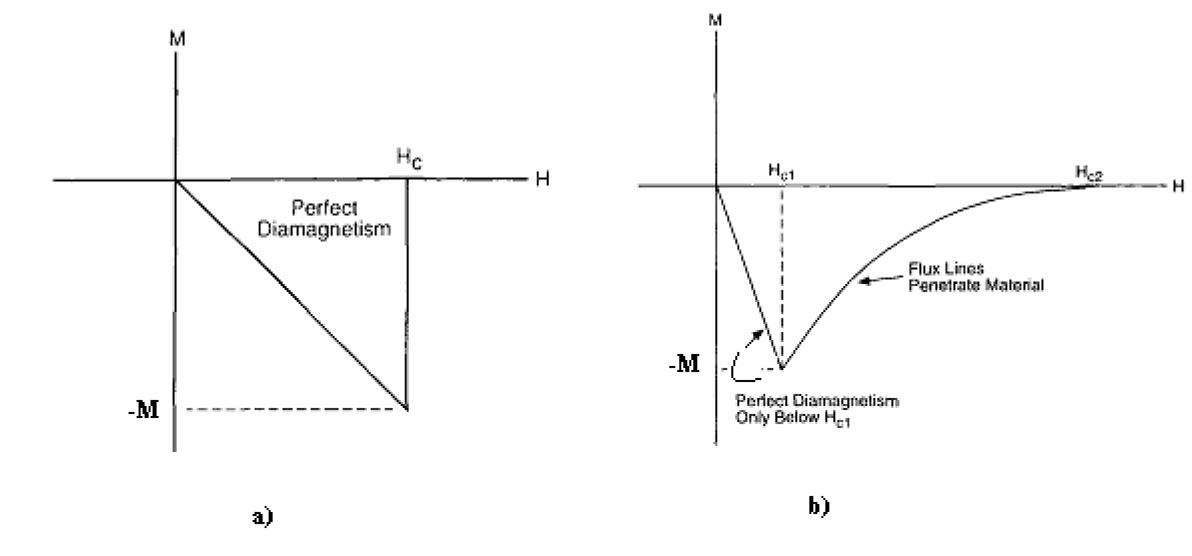

Figure 2.18 a) For a Type-I superconductor, magnetic flux is expelled ,producing a magnetization (M) that increases with magnetic field (H) is reached, at which it falls to zero as with a normal conductor. b) A Type-II superconductor has two critical magnetic fields (H_{c1} and H_{c2}) ; below H_{c1} Type –II behaves as type I , and above H_{c2} it becomes normal.

Just as superconductors have a critical temperature and a critical magnetic field so too do they have a critical current density as well. That there must be some upper limit to the current density J_c in a superconductor is required [31] by the relationship between current and magnetic field; for a wire of radius a carrying current I, the magnetic field at the surface $I/2\pi a$. The current cannot exceed the amount that produces a critical magnetic field H_c at the superconductor, which implies a critical current $I_c = 2\pi a H_c$ and $J_c = 2H_c / a$ for real superconductors, the actual critical current density is less than this upper limit and the actual current is limited by other physical mechanisms [32].

For a Type-I superconductor, critical current is simply a consequence of the critical magnetic field Since is low in Type-I superconductors, their critical current densities are likewise low. This is why Type-I superconductors have not been of interest to the electric utilities or magnet builders. In a Type-II superconductor, the relationship is much more complicated; indeed, Figure 2.19 shows the critical surface in the 3-dimensional space of temperature, magnetic field, and current (TBJ) [33] . This is known as a THJ plot, after the three axes. The critical current is no longer related in a trivial way to the magnetic field.

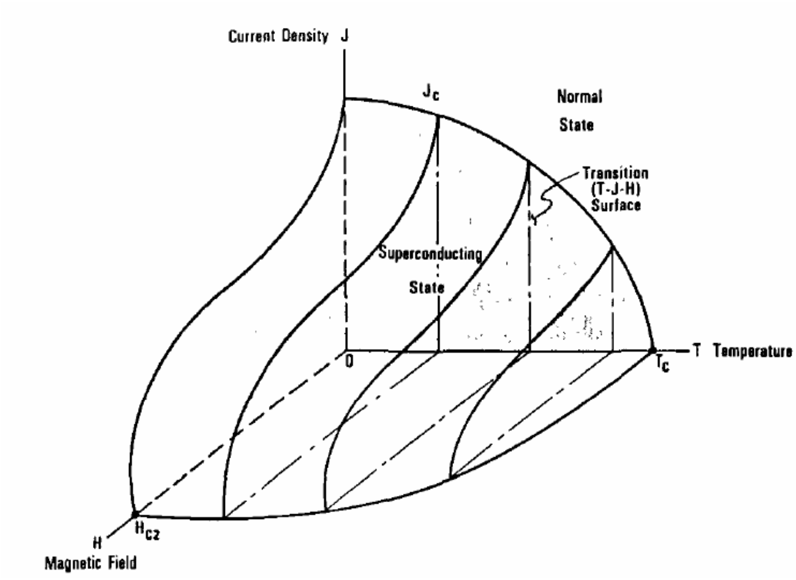

Figure 2.19 The relationship between, magnetic field, and critical current in a superconductor. Anywhere inside the surface, the material is superconducting.

2.8 High Temperature superconductors

In 1986 physicists Bednorz and Müller [10], firstly discovered superconductivity in a lanthanum-based cuprate perovskite material, T_c is about 35 K. . Bednorz and Muller observed evidence of superconductivity with transition temperature over 30K in $La_{2-x}Ba_xCuO_4$. This material had perovskite structure.

After ,the replacing the lanthanum with yttrium ,making YBCO ,raised the critical temperature to 92 K by Wu et al [34], this high T_c superconductors are oxide superconductors, with perovskite structure. Before their discovery superconductivity was unknown in copper oxides A substitution of yttrium for lanthanum led to the discovery of $YBa_2Cu_3O_{6+\delta}$ ($\delta < 1$) often referred to as YBCO or 123 because of the ratio of Y:Ba:Cu in this material. This was the first superconductor discovered with a T_c in the range 90-95K, [33] well above the boiling point of liquid nitrogen.

This discovery was followed in 1988 by the discovery of bismuth ($Bi_2Sr_2Ca_2Cu_3O_{10+\delta}$) and thallium ($Tl_2Ba_2Ca_2Cu_3O_{10+\delta}$) based superconductors with even higher T_c. A large family of these superconductors with over 40 members is now known.

BSCCO families of superconductors have also perovskite type structure with copper oxide planes and chains and orthogonal unit cells. Two most common members are $Bi_2CaSr_2Cu_2O_{8+\delta}$ ($\delta < 1$) commonly known as 2212 or 85K phase, and $Bi_2CaSr_2Cu_3O_{10+\delta}$ commonly known as 2223 or 110K phase. Thallium superconductors have similar structure. The highest T_c in this family is 125K. With the increasing number of CuO planes the T_c seems to increase in the oxide superconductor family [35].

After the discovery of high T_c superconductors, they have been subjected to intense investigations to determine microstructure present in them using transmission electron microscopy and related techniques. Relations between structure, microstructure and normal and superconducting properties have also been determined in many cases. Of course, as in conventional superconductors the microstructure present in oxide superconductors is expected to play a prominent role in determining the current carrying capacity of these materials. It is now known that the important defects in these superconductors include twin and grain boundaries.

The BCS theory explains quite successfully some properties of superconductors at low temperature that is near the absolute zero above about 30 K whereas it is not successful enough to explain the theoretical explanation of high Tc superconductors and their phenomena.

2.9 BSCCO System

The Bi-Sr-Ca-Cu-O (BSCCO) system a new high Tc oxide superconductor was discovered by H. Maeda in 1988. T_c of the system is observed to be about 105 K higher than that of $YBa_2Cu_3O_7$. In this superconductor system, the coexistence of Sr and Ca is necessary to obtain high Tc [36].

There are three different phases (2201, 2212 and 2223) of the BSCCO system with respect to their chemical stoichiometric compositions. For BSCCO 2201 (also referred to"Bi-2201") an approximate transition temperature is 20 K, for BSCCO-2212 (also referred to"Bi-2212") the transition temperature is nearly 85 K, for BSCCO-2223 (also referred to "Bi-2223") an approximate transition temperature is determined to be 110 K. These different phases depending on the number of Cu-O layers in their crystal structure are clearly shown in Figure 2.20.

Within this type of superconductors there exist several superconducting phases which differ in their number of copper-oxide layers in the crystalline unit cell. The composition of the superconducting phases of this system is generally described by the ideal formula $Bi_2Sr_2Ca_{n-1}Cu_n$ where n=1,2,3 represents the number of copper-oxide layers. The most interesting phases are noticed to be n=2, 3 for technical applications.

The unit cells of these phases have a layer structure consisting of BiO double layers that alternate with perovskite-like $Sr_2Ca_{n-1}Cu_nO_{1-2n}$ units having also a layered structure with copper oxide sheets. respectively. The crystal parameters of the three phases are:

$$a=b= 5.4\ \overset{0}{A},\ c=24.4\ \overset{0}{A}\ \text{for 2201 phase}$$

$$a=b= 5.4\ \overset{0}{A},\ c=30.7\ \overset{0}{A}\ \text{for 2212 phase}$$

$$a=b= 5.4\ \overset{0}{A},\ c=37.1\ \overset{0}{A}\ \text{for 2223 phase}$$

The number of copper-oxide planes is closely related to Tc, it increases with the number of Cu-O layers. The 2201, 2212 phases are known as the low Tc phases. The 2223 phase is known as the high Tc phase.

Under normal preparatory conditions, the 2212 type appears to be the most stable and is often the most dominant in the presence even when the starting composition was aiming for 2223. The 2223 phase can be gradually stabilized with annealing just below the melting point. With 15 % of Bi replaced by Pb , the 2223 type can be prepared in pure form.

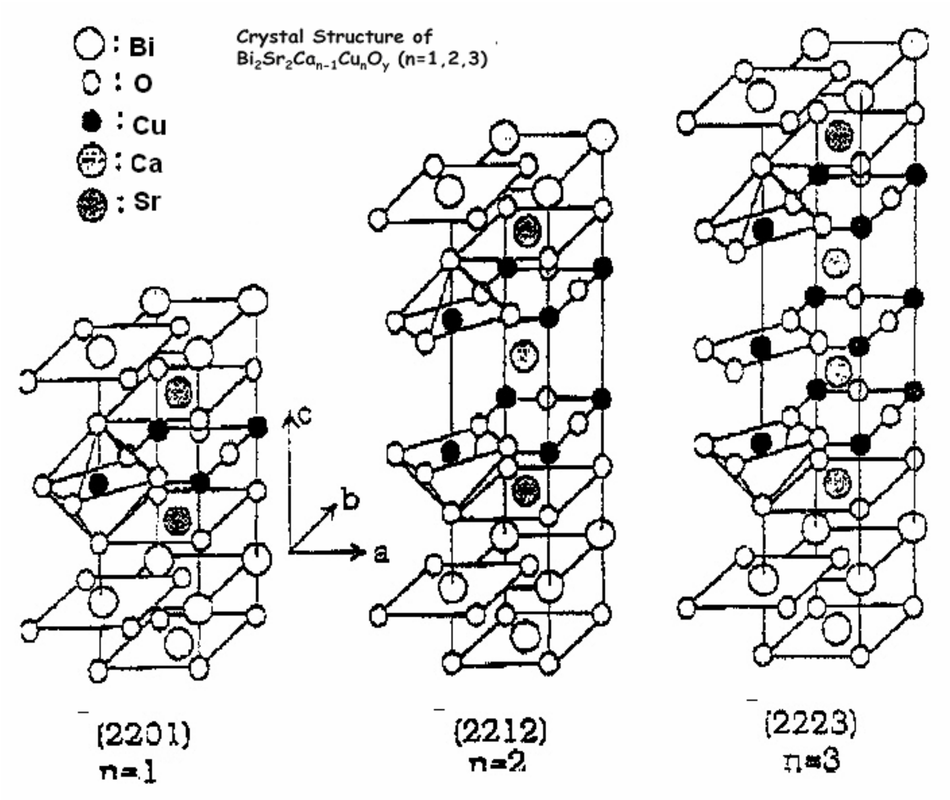

Figure 2.20. Crystal structure of BSCCO system

By Tc measurement alone, the individual member of the BSCCO family can be distinguished and studied separately. Therefore the BSCCO group provides the best opportunity to study the individual structure –related properties in the normal as well as superconducting states [37] .

Superconductivity in Bi- based system is studied by a large number of researchers, but to obtain good superconducting properties a careful processing is necessary. One advantage of the Bi- based system is that it does not contain poisonous elements unlike the Tl based superconductors.

Appropriate starting compounds for both the respective metal elements of the high temperature superconductor material of BSCCO-type as well as Ba as substituent of part of the proportion of Sr are metal oxides, hydroxides, carbonates, hydrates, oxalates or other reactive precursors, the metal oxides being preferred. The starting compounds may be produced by wet or dry mixing, by co precipitation of material from solution, or by any other method which results in intimate mixture of reactive particles.

According to the present invention in the desired BSCCO high temperature superconductor material the proportion of Sr which can be replaced by Ba, is preferably more than 5 at % and less than 50 at %.

According to a preferred embodiment of the present invention the high temperature superconductor material of BSCCO-family has a nominal composition of $Bi_{2-x}Sr_{2-y}Ba_{y}Ca_{1-z}Cu_{2}O_{8}$ with $0 \leq x < 0.4$, $0.05 < y < 0.5$ and $0 < z < 0.2$. Further, Bi can be replaced by Pb in a proportion of up to 22 at %.

The homogeneity of the critical current could be improved from variation of about 30% in the corresponding non substituted superconductor materials to a value of only 5% or even less. In addition, the critical current itself could be increased up to 20%. By applying the starting composition of the present invention to a centrifugal melt casting process it is possible to produce cylindrically shaped superconductor bodies such as rods tubes, having a diameter of 5 mm and a length of about 300 mm which do not bend during annealing. The present invention is particularly useful for obtaining shaped bodies with substantially round cross-sections such as shaped bodies with tubular or annular shapes, e.g. rods, tubes etcetera.

CHAPTER 3

EXPERIMENTAL TECHNIQUES

3.1 Sample Preparation

Superconducting BiPbSrCaCuO samples were prepared by the standard solid-state reaction method. The weighed commercially available powders from Alfaaesar Company of Bi_2O_3 (99.99%), PbO (99.9+%), $SrCO_3$ (99.9+%), $CaCO_3$ (99+%) and CuO (99+%) in the stichometry ratio of Bi:Pb:Sr:Ca:Cu = 1.8:0.35:1.9:2.1:3 were mixed by grinding machine for 24 h. The mixed powders were calcined in air at 800 ^{o}C for 12 hours.

Figure 3.1 Three zone tube furnace

Heat treatment was performed with the help of three zone tube furnace (Figure 3.1)

After calcinations process, the powders were cooled to room temperature in order to regrind. The regrind materials were reground and pressed into pellets of 10x4x2 mm^3 at 300 MPa. The pellets were sintered in air at 845 ^oC for 48 h and then cooled down to room temperature with different cooling rates by means of simple system (Figure 3.2) designed in Material Research Laboratory, Abant Izzet Baysal University. As seen from Figure 3.2 step motor controlled by a personal computer pulls the Cu wire, which is connected to the Al crucible holding the sample in the tube furnace. The cooling rates were determined to be 273°C/minute, 136°C/minute, 55°C/minute, 25°C/minute, and 18°C/minute. Furnace cooling (5°C/minute) and fast cooling (quenched in air) were also worked.

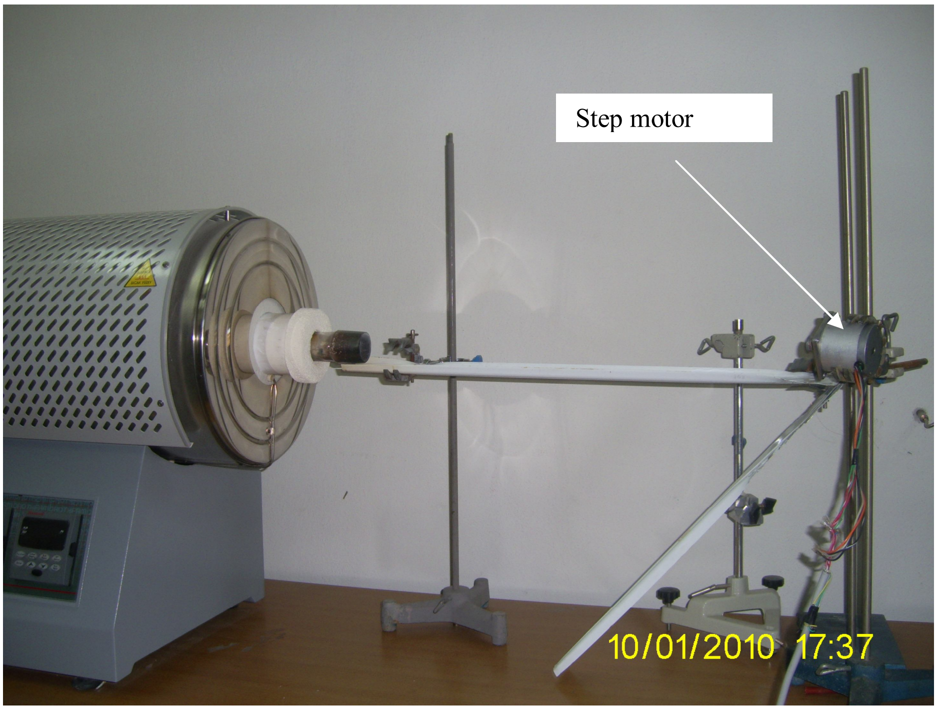

Figure 3.2 System for controlled sample cooling

In this thesis, resistivity versus temperature measurements of the samples performed at 60-200 K by the help of crycooler system from CRYO INDUSTRIES were carried out by standard four-point method. Both the current and voltage contacts were made by high conductive silver paint. The outer and inner contacts were chosen for current and voltage, respectively. 10 mA current was biased for all the transport resistivity measurements.

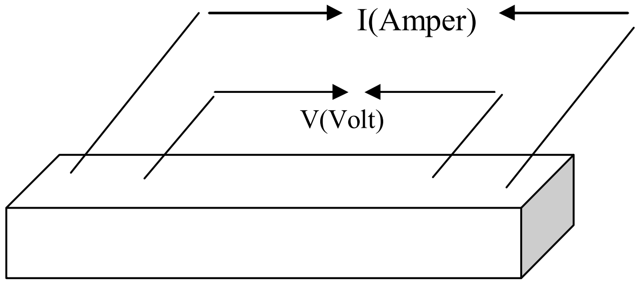

Figure 3.3- Transport critical current measurement.

Transport critical current density measurements, $J_{c,}$ of the samples were performed by using home-made system in liquid nitrogen (77 K) with the same resistivity measurement contacts. After immersed into liquid nitrogen, the sample on the sample holder was waited for temperature stabilization for a few minutes. Current step applied to samples was adjusted to be 0.1 A during the critical current measurements. When J_c was determined critical current criterion was chosen to be 1 mV/cm.

Figure 3.4 Closed loop 4 K gas contact crycooler

The surface morphology and microstructure of the materials were analyzed by scanning electron microscopy (SEM), JEOL 6390-LV (Fig. 3.4). The magnifications to get information about the grains clearly were adjusted to be 1000 and 3000.

Figure 3.5 Scanning electron microscopy

X-ray powder diffraction (XRD) patterns were obtained by means of the Rigaku, Multiflex (Fig. 3.5) diffractometer (Cu K_{α}) in the range $2\Theta = 3°- 60°$ at 40 kV and 30 mA with a scan speed of 3° /min and a step increment of 0.02°

Figure 3.6 X-RAY diffractometer

CHAPTER 4

RESULTS AND DISCUSSION

Figure 4.1 shows resistivity versus temperature graph for the samples annealed at 845°C with 273°C/minute, 136°C/minute, 55°C/minute, 25°C/minute, 18°C/minute cooling rates, furnace cooling (approximately 5°C/minute) and fast cooling (quenched in air). As seen from the graphs, critical temperatures (ρ =0), T_c, are found to be about 102 K, 112 K, 104 K, 113 K, 105 K, 102 K and 102 K for the samples with 273°C/minute, 136°C/minute, 55°C/minute, 25°C/minute, 18°C/minute cooling rates, furnace cooled and quenched in air, respectively. In addition, the resistivity is found to be about 5.2 mΩ.cm at 140 K for the sample obtained with 845°C/minute cooling rate and transition width is noted to be about 13 K. Furthermore, as known from the literature, a kink on the ρ-T graphs can be appeared during transition to zero resistivity . In this study, even though the kinks are observed for samples obtained with 273°C/minute cooling rate, furnace cooling and quenched in air, prominent effect on T_c of cooling rates was not observed.

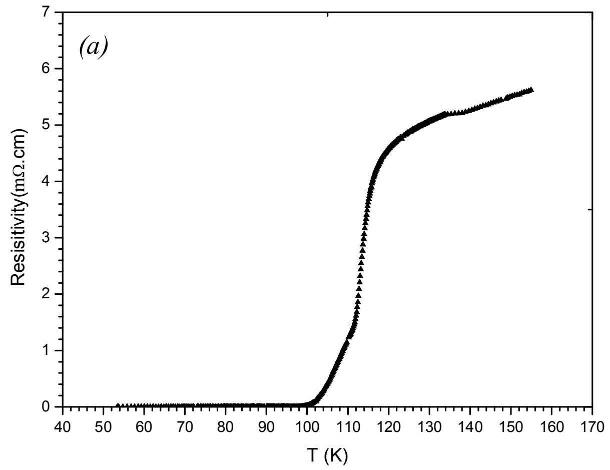
(a)
Resisitivity(mΩ.cm)
T (K)

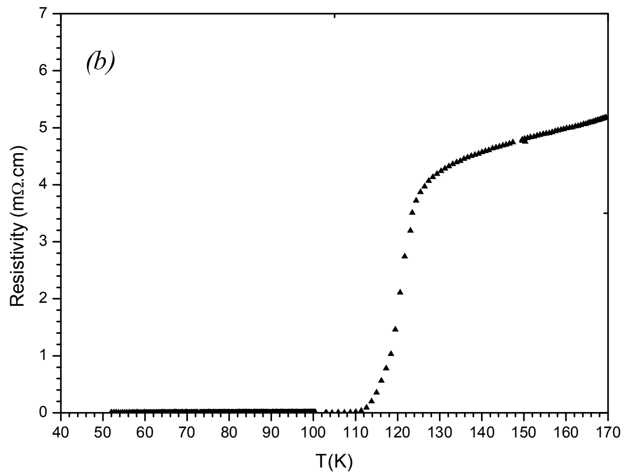
(b)
Resistivity (mΩ.cm)
T(K)

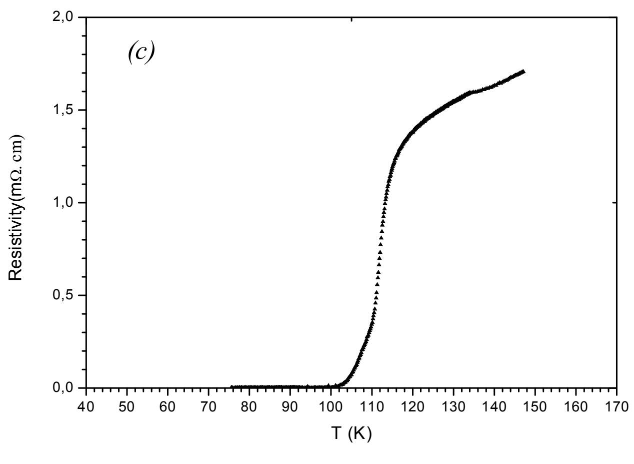
(c)
Resistivity(mΩ. cm)
T (K)

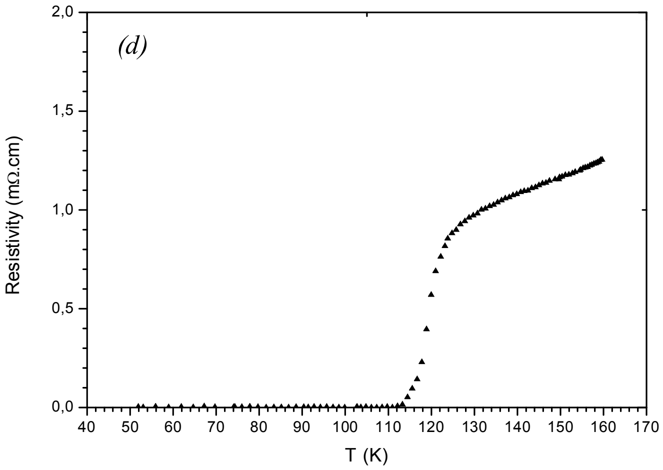

(d)
Resistivity (mΩ.cm)
2,0
1,5
1,0
0,5
0,0
40 50 60 70 80 90 100 110 120 130 140 150 160 170
T (K)

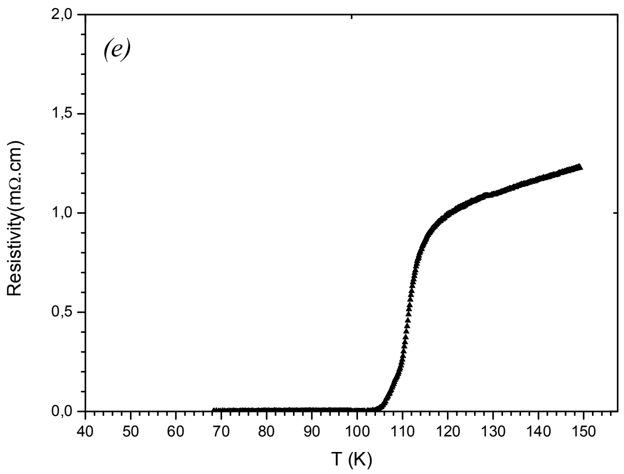

(e)
Resistivity(mΩ.cm)
2,0
1,5
1,0
0,5
0,0
40 50 60 70 80 90 100 110 120 130 140 150
T (K)

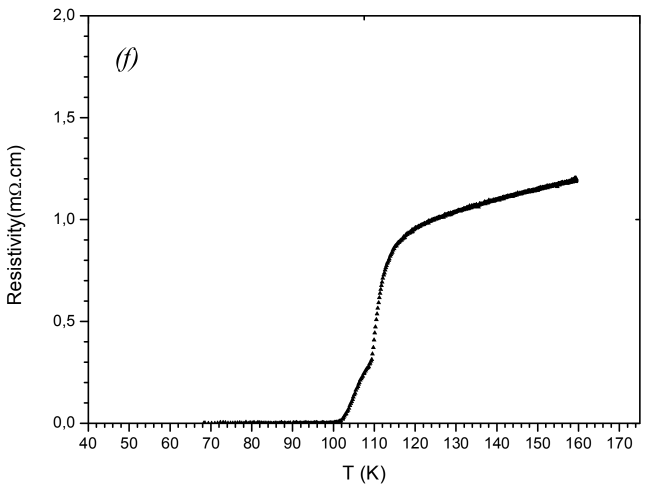

(f)
Resistivity(mΩ.cm)
2,0
1,5
1,0
0,5
0,0
40 50 60 70 80 90 100 110 120 130 140 150 160 170
T (K)

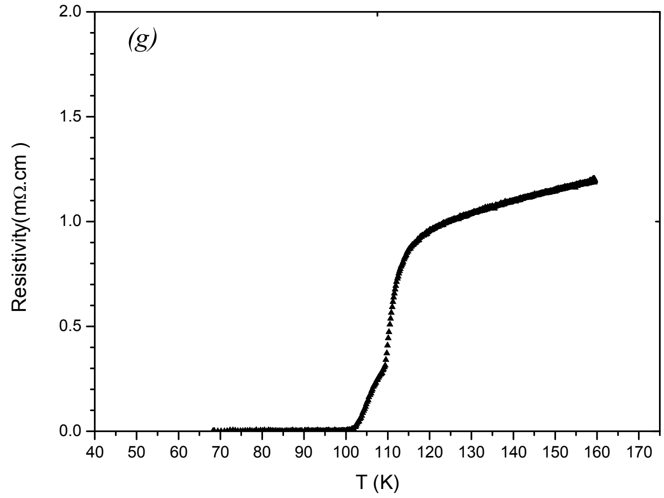

Figure 4.1 Resistivity versus temperature graph for the samples annealed at 845°C with (*a*) 273°C/minute , (b) 136°C/minute, (c) 55°C/minute, (d) 25°C/minute, (e) 18°C/minute cooling rates, (f) furnace cooled and (g) quenched in air.

X-ray diffraction patterns of samples were depicted in Figure 4.2. The characteristic peaks of Bi-2212 and Bi-2223 phases are found to be 5.7, 23.2, 27.5 and 4.7, 23.9, 28.8, 33.8, respectively. As can be seen from the Figure 4.2 (a, b,d and g parts), (*hk*l)*H* peaks were found to be more predominant than (*hk*l)*L* peaks. The volume fractions were also calculated by following equations

$$f_{(2223)} = \frac{\sum I_{H(hkl)}}{\sum I_{H(hkl)} + \sum I_{L(hkl)}} \tag{4.1}$$

$$f_{(2212)} = \frac{\sum I_{L(hkl)}}{\sum I_{H(hkl)} + \sum I_{L(hkl)}} \tag{4.2}$$

Here $I_{H(hkl)}$ and $I_{L(hkl)}$ are the intensities of the (*hkl*) diffraction lines for Bi-2223 and Bi-2212 phases, respectively. As the result of XRD measurements, the following consequences are obtained.

Table 4.1-The volume fractions of Bi-2212 and Bi-2223 phases , Tc and Current Density of Samples

The sample	Volume fraction of Bi-2212	Volume fractions of Bi-2223	T_c (K) at ρ =0	Critical Current Density (J_c at 77 K) (A/cm^2)
quenched in air	48	52	102	9
273°C/minute	42	58	102	15
136°C/minute	42	58	112	23
55°C/minute	68	32	104	28
25°C/minute	44	56	112	27
18°C/minute	53	47	105	43
furnace cooled	52	48	102	51

As seen from Table 4.1, the sample quenched in air , at 273°C/minute, 136°C/minute, 25°C/minute cooling rate showed higher volume fraction of Bi-2223 phase than Bi-2212 phase. According to the table, 273°C/minute and 136°C/minute cooling rates are found to be the optimum values to obtain Bi -2223 phase. Critical transition temperature and transport critical current density (J_c) of sample obtained with 136°C/minute cooling rate are noted to be 112 K and 23 A/cm^2 at 77 K (liquid nitrogen temperature), respectively. Moreover, highest J_c is observed to be about 51 A/cm^2 for the sample cooled by the furnace. It is obviously seen that J_c increases with decreasing the cooling rates.

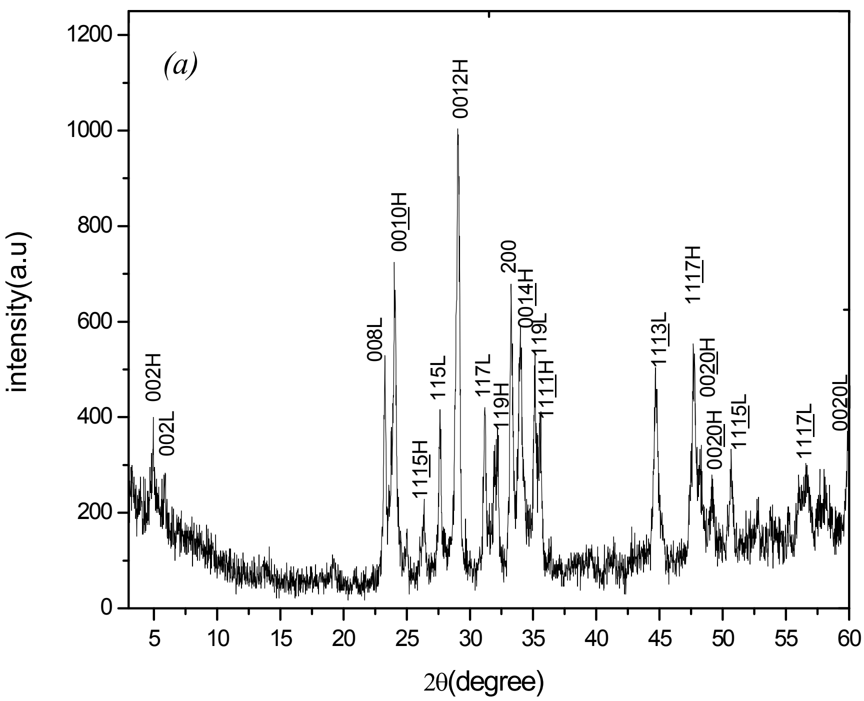
(a)
intensity(a.u)
2θ(degree)
002H
002L
008L
0010H
1115H
115L
0012H
117L
119H
200
0014H
119L
1111H
1113L
1117H
0020H
0020H
1115L
1117L
0020L

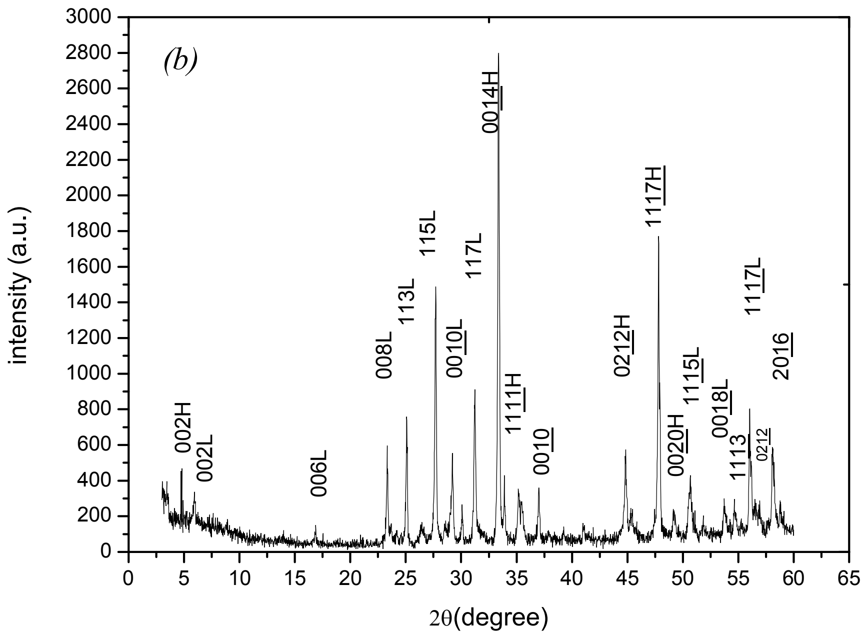
(b)
intensity (a.u.)
2θ(degree)
002H
002L
006L
008L
113L
115L
0010L
117L
0014H
1111H
0010
0212H
1117H
0020H
1115L
0018L
1113
0212
1117L
2016

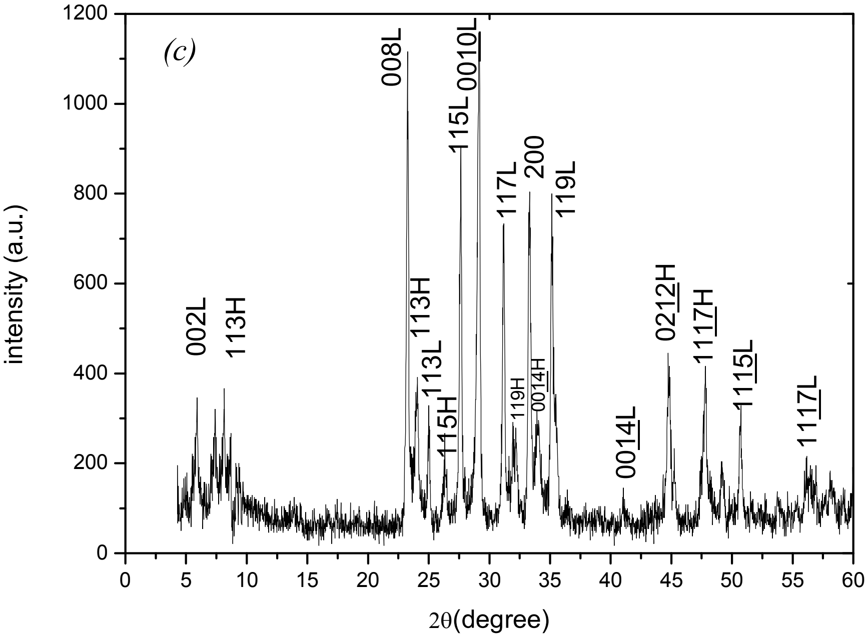
(c)
intensity (a.u.)
2θ(degree)
002L
113H
008L
113H
113L
115H
115L
0010L
117L
119H
200
0014H
119L
0014L
0212H
1117H
1115L
1117L

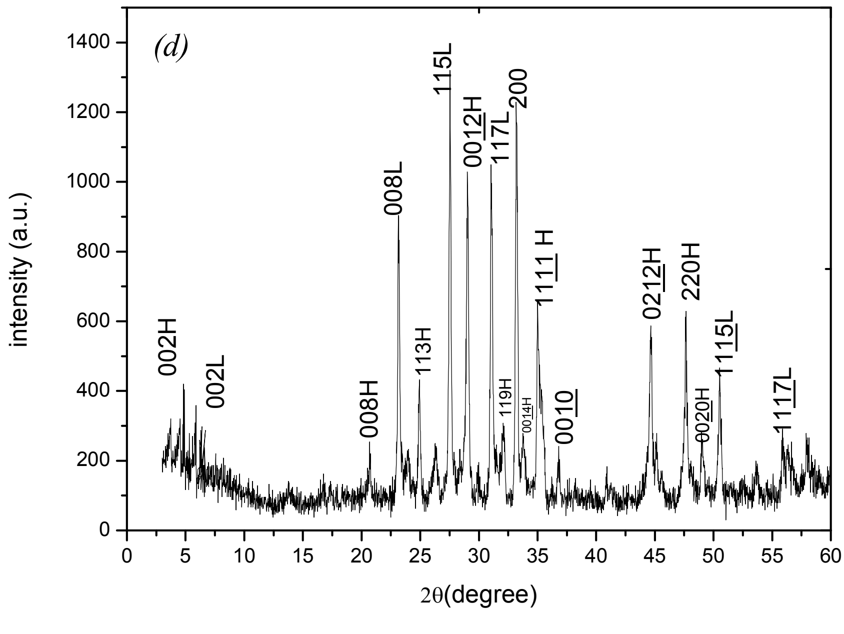
(d)
intensity (a.u.)
2θ(degree)
002H
002L
008H
008L
113H
115L
0012H
117L
119H
200
0014H
1111 H
0010
0212H
220H
0020H
1115L
1117L

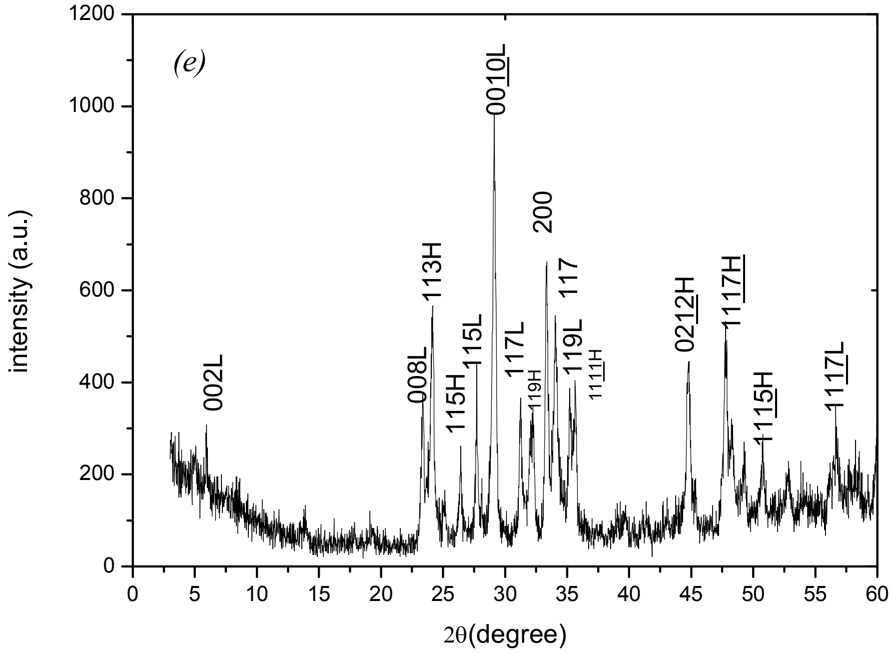
(e)
intensity (a.u.)
2θ(degree)
002L
008L
113H
115H
115L
0010L
117L
119H
200
117
119L
1111H
0212H
1117H
1115H
1117L

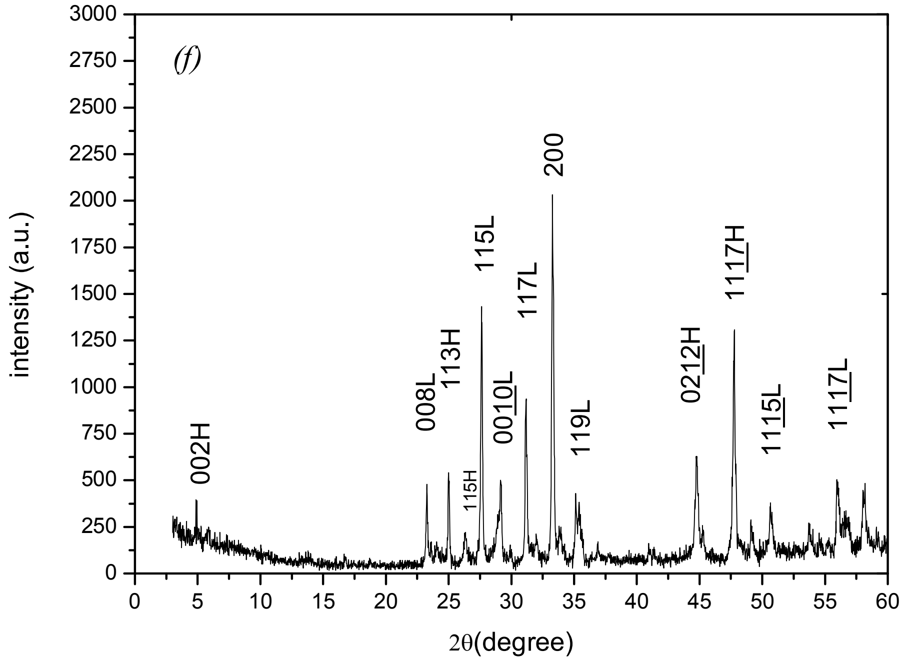
(f)
intensity (a.u.)
2θ(degree)
002H
008L
113H
115H
115L
0010L
117L
200
119L
0212H
1117H
1115L
1117L

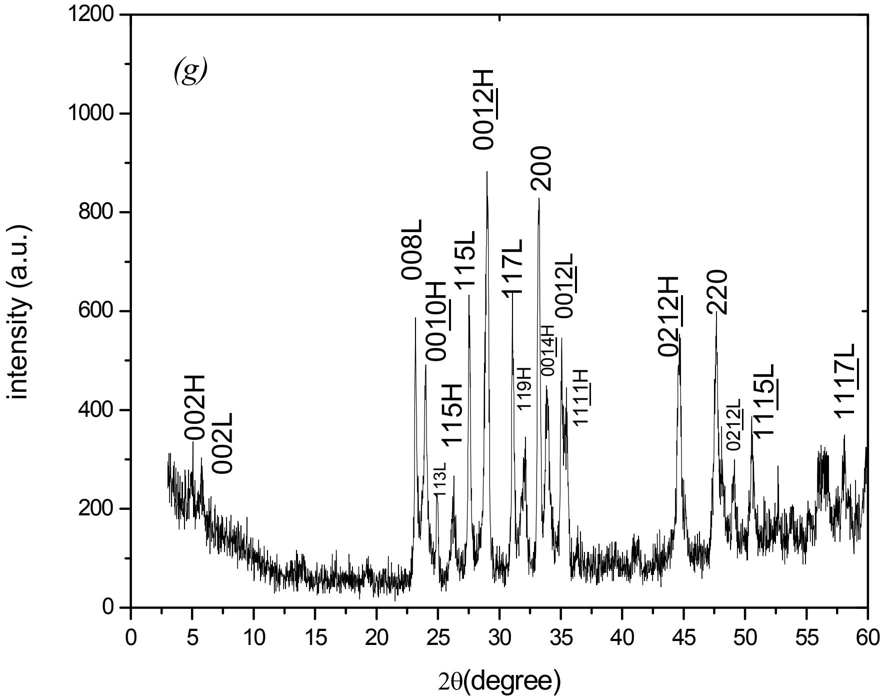

Figure 4.2 X-ray diffraction patterns for the samples annealed at 845°C with (*a*) 273°C/minute , (b) 136°C/minute , (c) 55°C/minute, (d) 25°C/minute, (e) 18°C/minute cooling rates, (f) furnace cooled and (g) quenched in air.

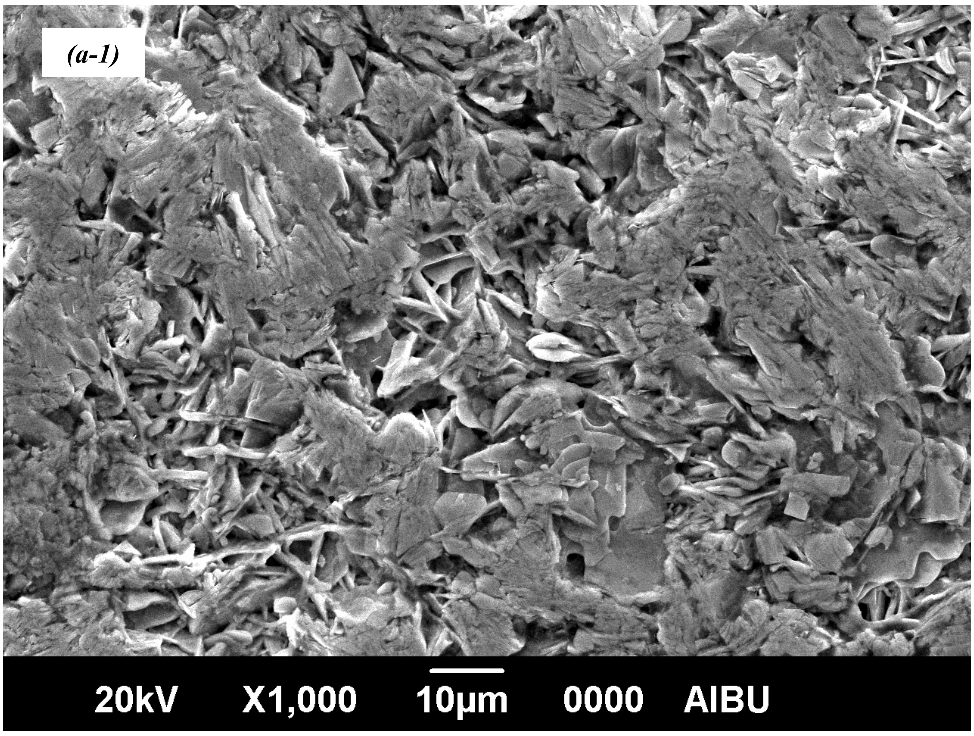
(a-1)
20kV X1,000 10μm 0000 AIBU

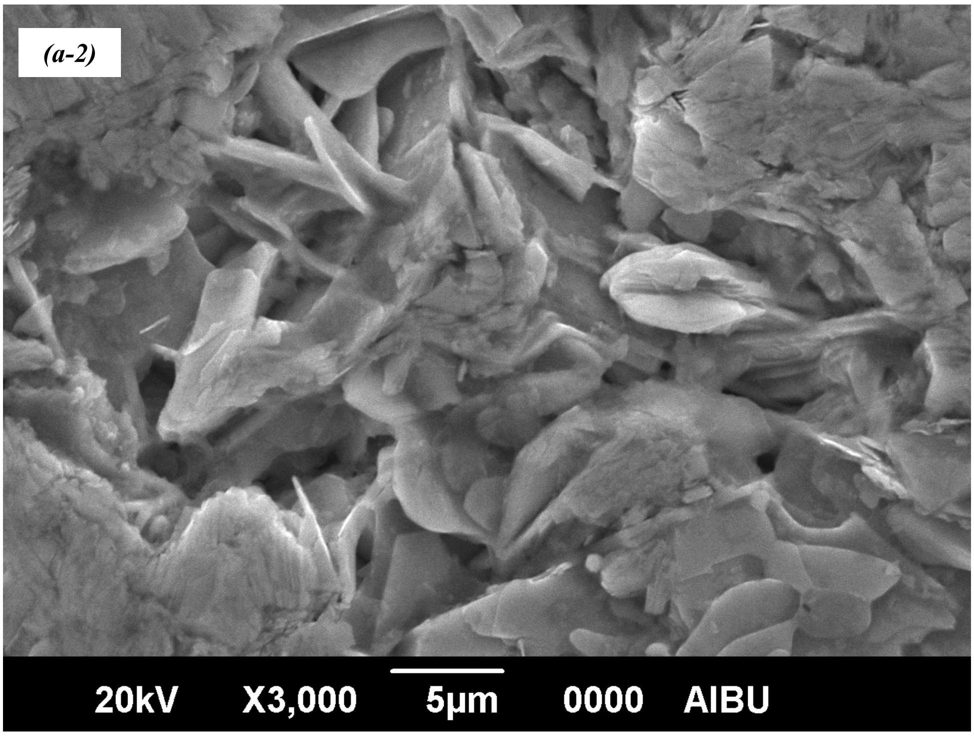
(a-2)
20kV X3,000 5μm 0000 AIBU

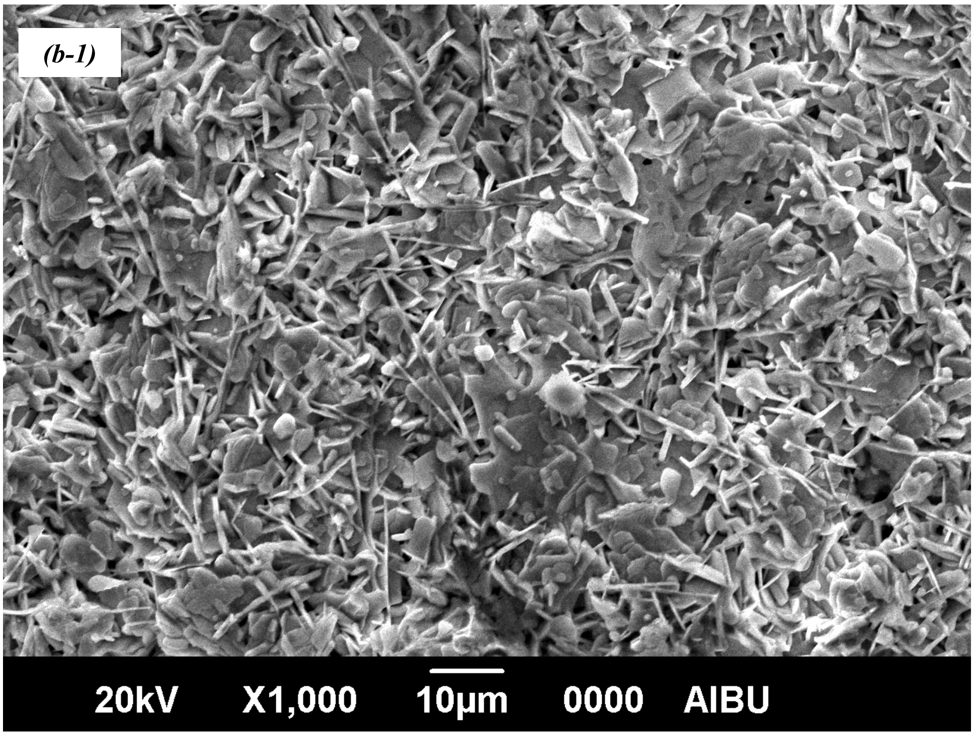
(b-1)
20kV X1,000 10μm 0000 AIBU

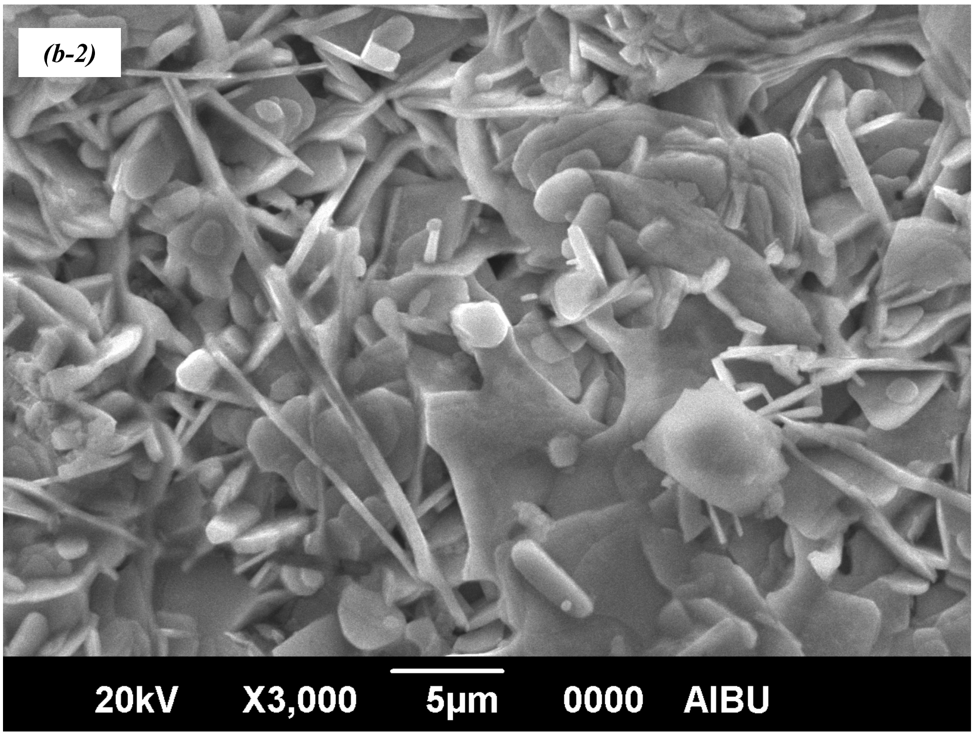
(b-2)
20kV X3,000 5μm 0000 AIBU

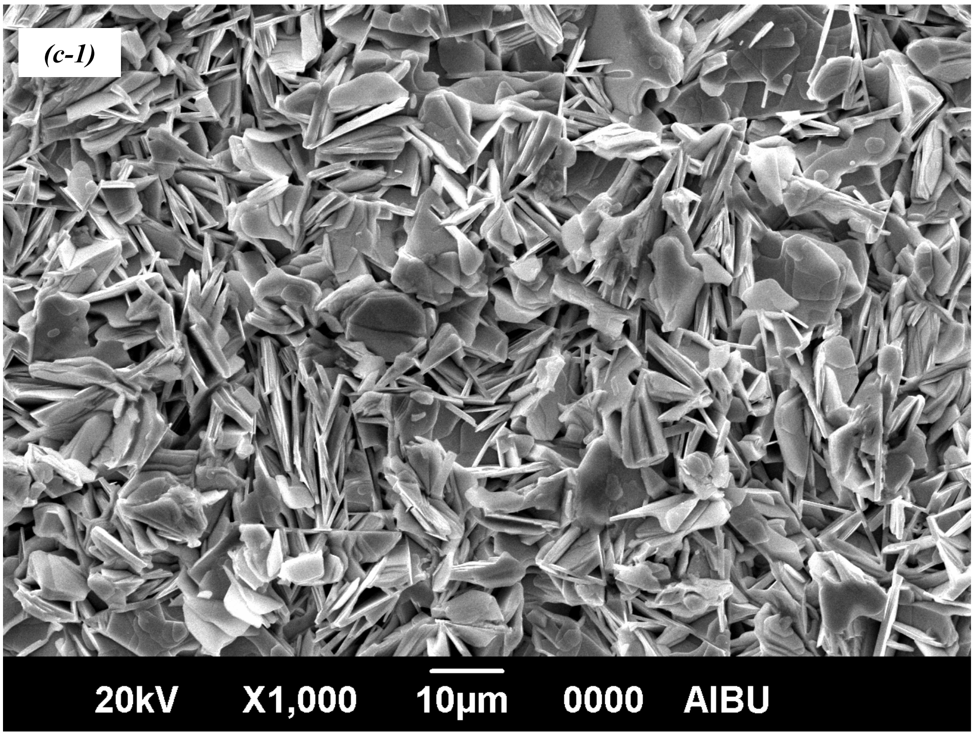
(c-1)
20kV X1,000 10μm 0000 AIBU

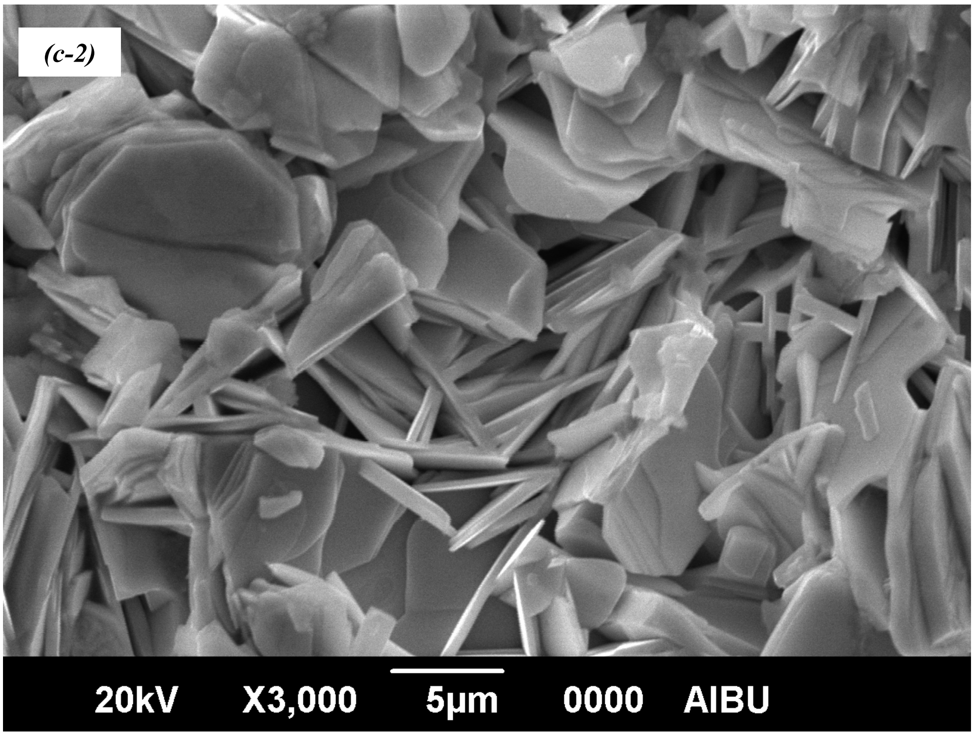
(c-2)
20kV X3,000 5μm 0000 AIBU

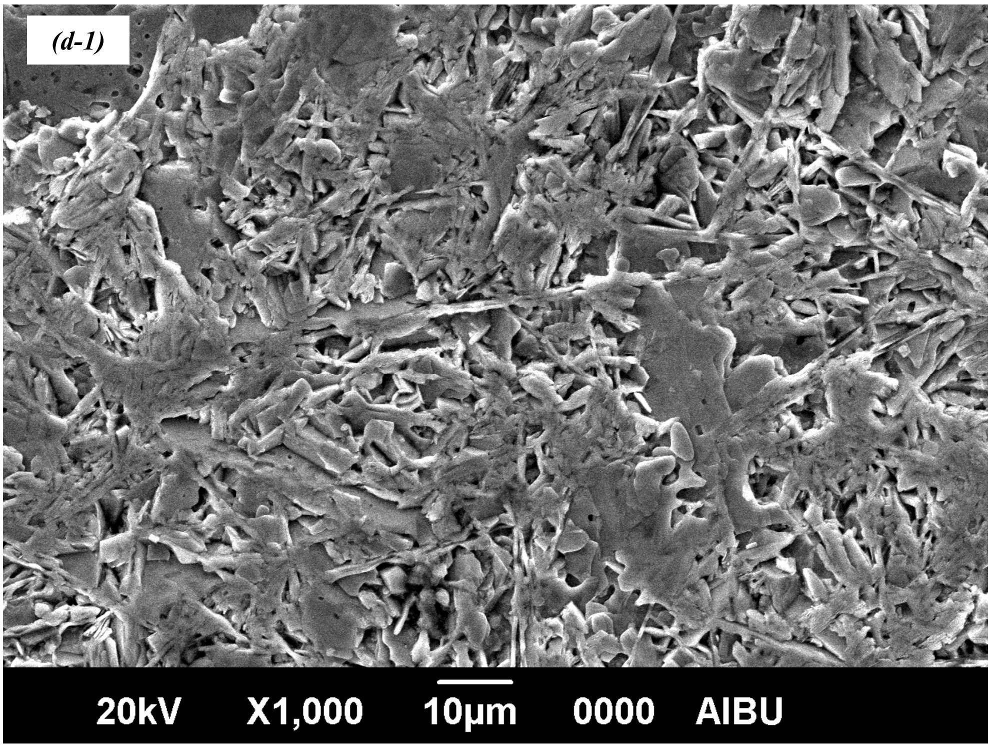
(d-1)
20kV X1,000 10μm 0000 AIBU

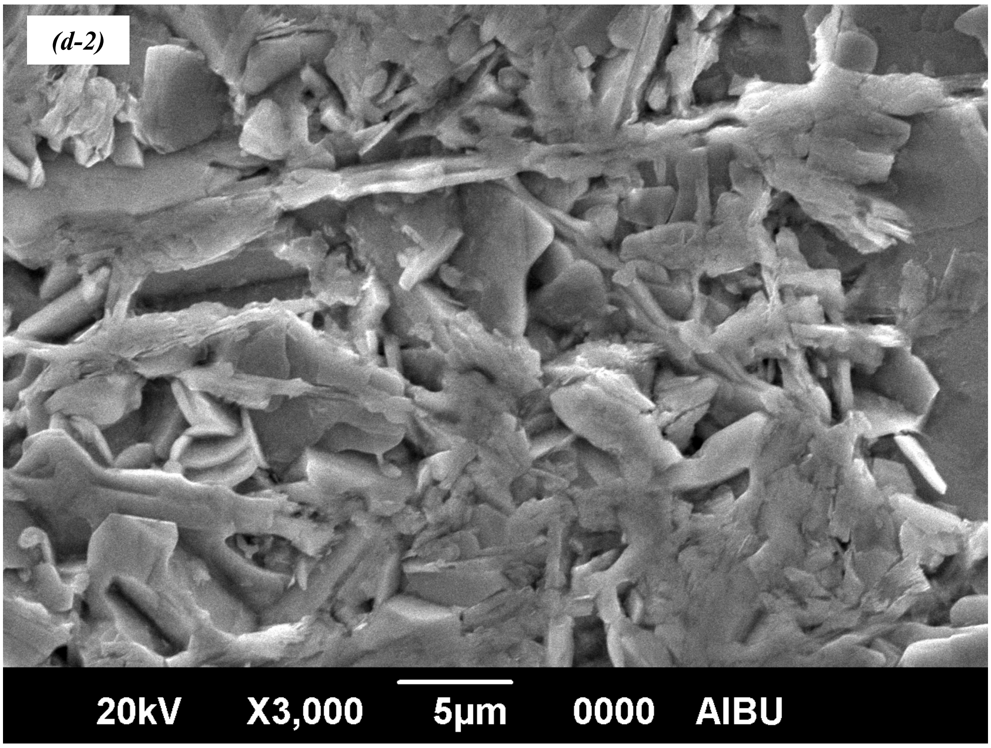
(d-2)
20kV X3,000 5μm 0000 AIBU

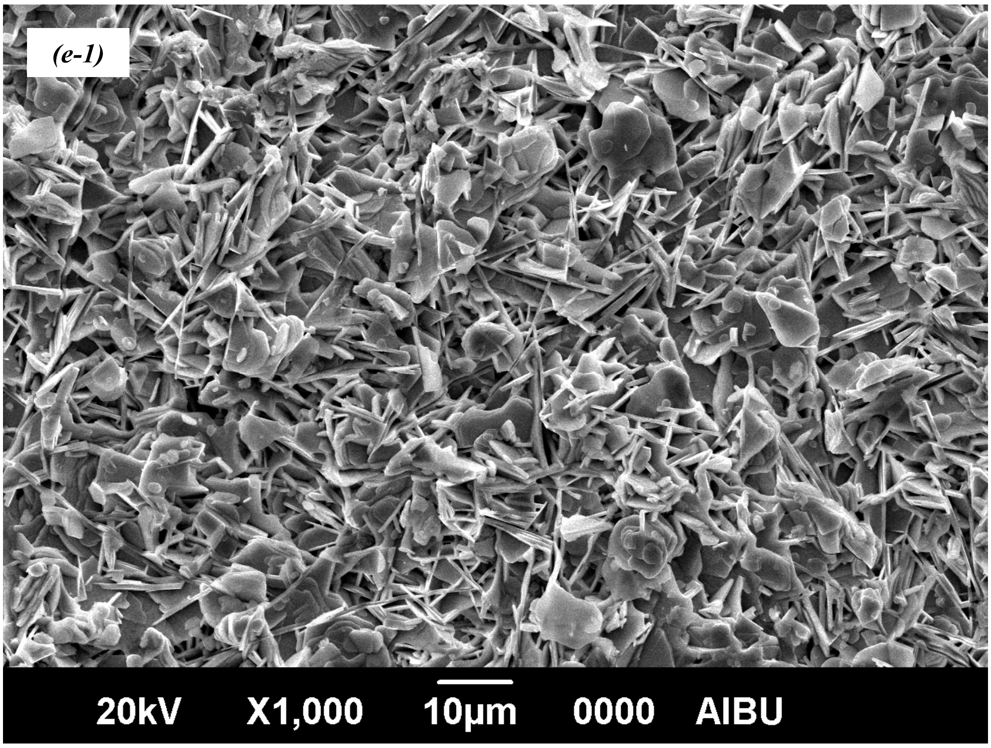
(e-1)
20kV X1,000 10μm 0000 AIBU

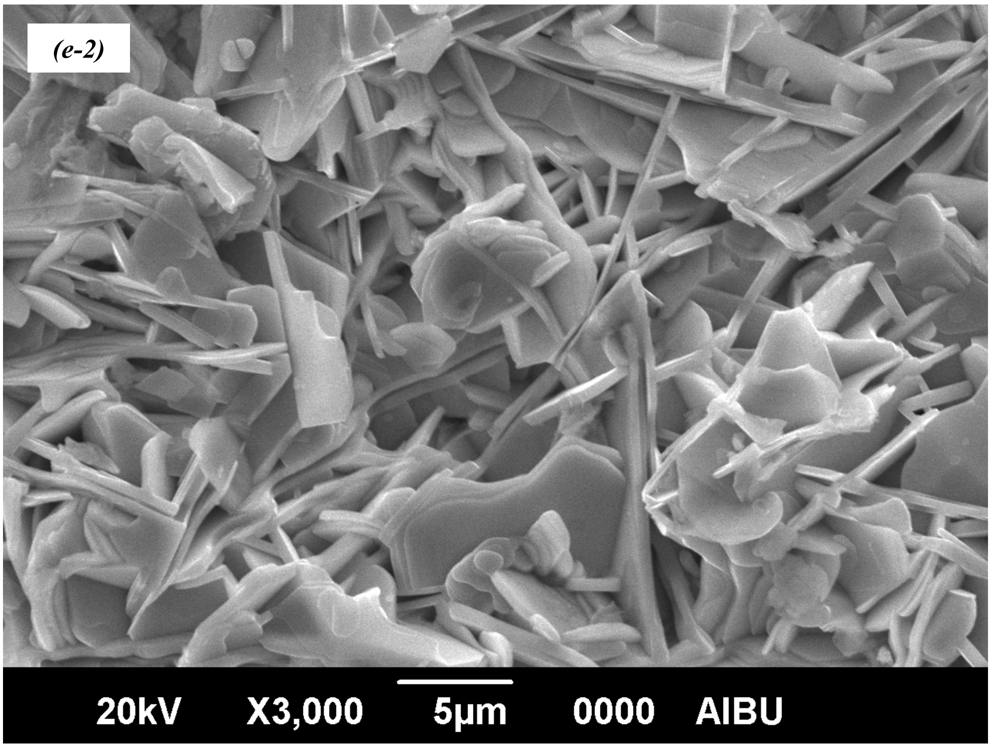
(e-2)
20kV X3,000 5μm 0000 AIBU

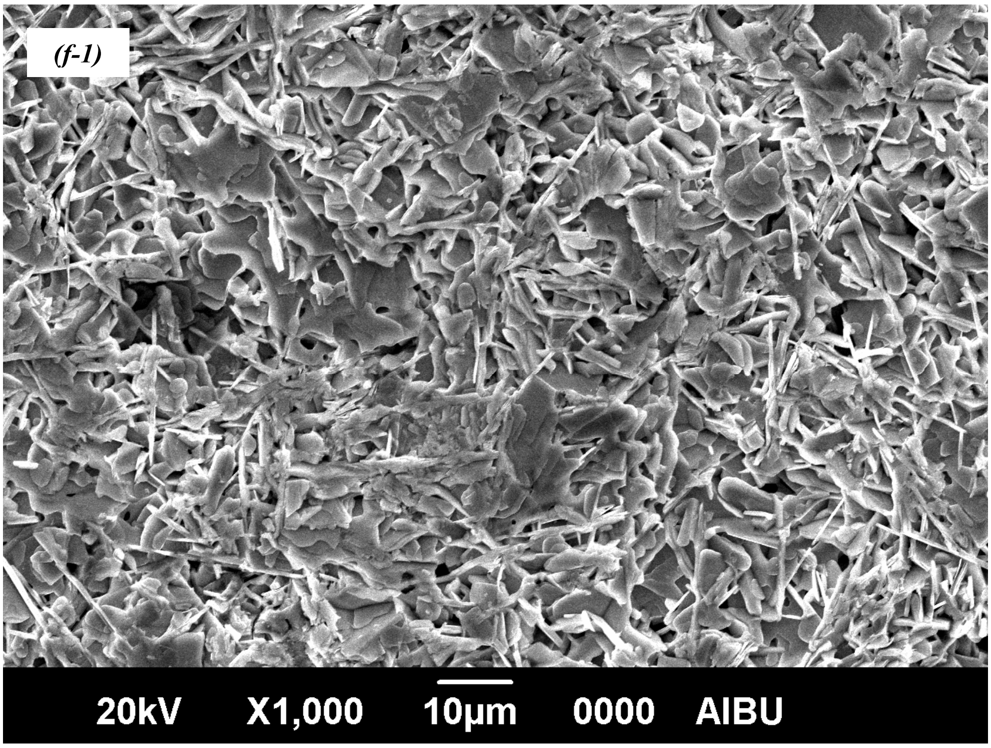
(f-1)
20kV X1,000 10µm 0000 AIBU

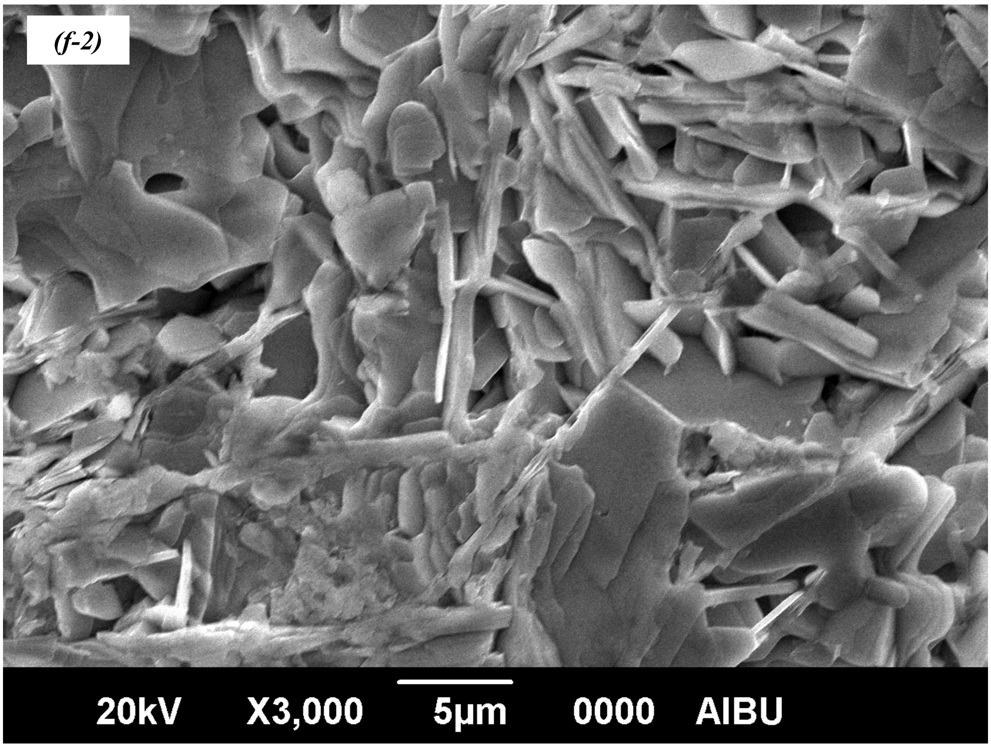
(f-2)
20kV X3,000 5µm 0000 AIBU

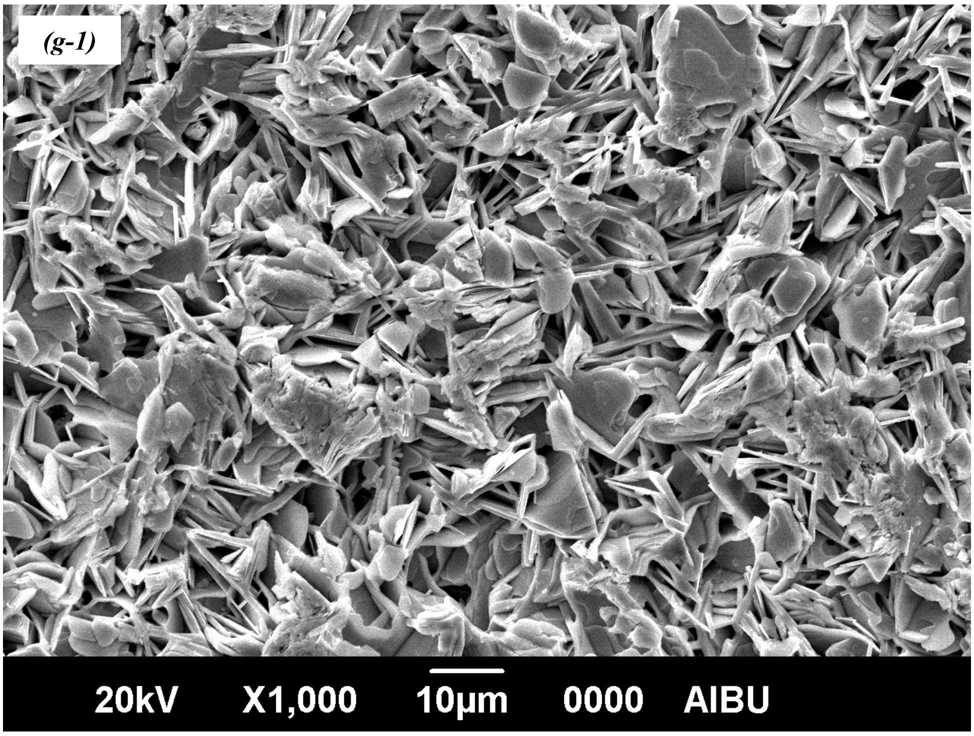
(g-1)
20kV X1,000 10μm 0000 AIBU

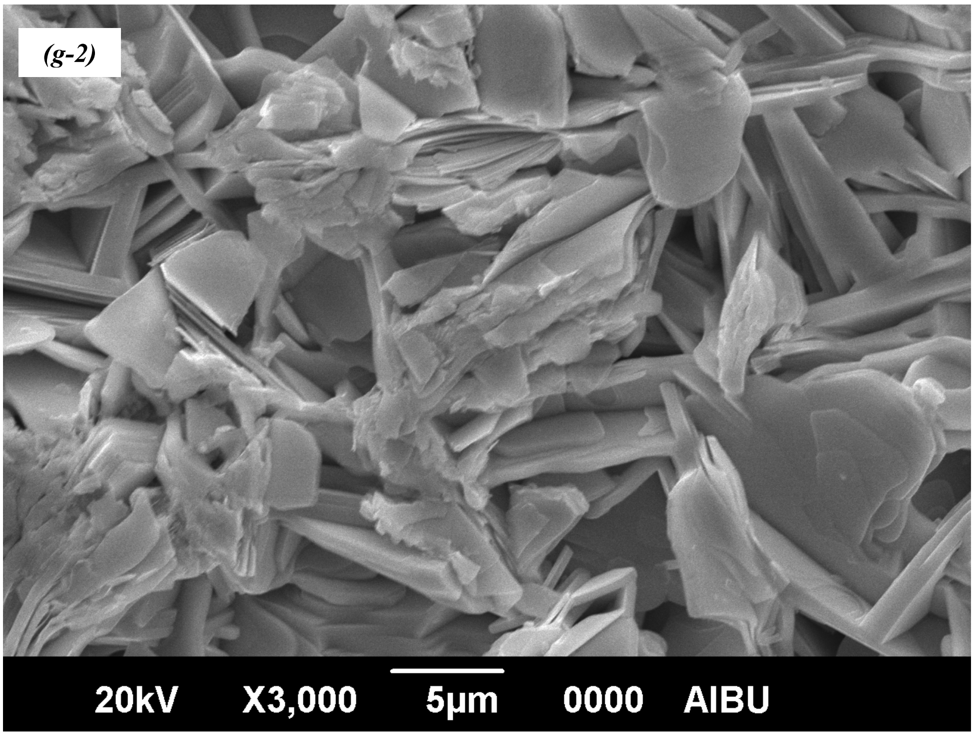
(g-2)
20kV X3,000 5μm 0000 AIBU

Fıgure 4.3- SEM micrographs of the different cooling rates for quenched in air ; (a-1)and (a-2) , for 273°C/minute; (b-1)and (b-2) , for 136°C/minute ;(c-1) and (c-2) , for 55°C/minute ; (d-1)and (d-2), for 25°C/minute ; (e-1)and (e-2) , for 18°C/minute ; (f-1) and (f-2) ; for furnace cooled ; (g-1) and (g-2) for magnified 1000 times and 3000 times

SEM micrographs for all the samples were shown in Figure 4.3. As seen from the photos, niddle-like and flake-like grains are appeared. But, flake-like grains are dominant in all samples. The sample prepared with 136 ^{o}C/min cooling rate (Figure 4.3 c) has the densier grain than the others. The grain size of the sample with 136 ^{o}C/min cooling rate is considerably larger than the others. This is consistent with critical temperature measurements.

CHAPTER 5

CONCLUSION

We have investigated the effect of the different cooling rates on BSCCO. The cooling rates were determined to be 273°C/minute, 136°C/minute, 55°C/minute, 25°C/minute, and 18°C/minute. Furnace cooling (5°C/minute) and fast cooling (quenched in air) were also worked. Resistivity versus temperature measurements of the samples performed at 60-200 K. According to the results prominent effect on T_c of cooling rates was not observed. Transport critical current density measurements, J_c, of the samples were performed and highest J_c is observed to be about 51 A/cm^2 for the sample cooled by the furnace. As an important result It is obviously seen that J_c increases with decreasing the cooling rates. X-ray powder diffraction (XRD) patterns were obtained and the volume fractions were calculated for Bi-2223 and Bi-2212 phases. The sample quenched in air, at 273°C/minute, 136°C/minute, 25°C/minute cooling rates showed higher volume fraction of Bi-2223 phase than Bi-2212 phase. The surface morphology and microstructure (SEM) of the materials were analyzed. Flake-like grains are dominant in all samples but the sample prepared with 136 ^{o}C/min cooling rate has the densier grain than the others. This is a suitable condition for the critical temperature is higher.

REFERENCES

[1] Kittel ,C.,Introduction to Solid State Physics, John Wiley

[2] Meissner ,W.Ochsenfeld, R.,, *Naturwiss.* **21,** 787 (1933). (1933)

[3] F. and H. London, *Proc. Royal Soc. A* **149**, 71 (1935); and F. London, *Superfluids,* Vol. I (Wiley, New York:1950)

[4] V.L. Ginzburg, L.D. Landau, J.Exptl. Theoret. Phys. (U.S.S.R) **20**, 1064 (1950)

[5] Abrikosov, A.A. *Zh. Eksp. Teor. Fiz.* **32**, 1442 (1957) ,Dokl. Akad. Nauk SSSR **86**, 489 (1952)

[6] J. Bardeen, L.N. Cooper, J.R. Schrieffer, Department of Physics,University of Illinois,Urbana, Illinois ,Phys.Rev. 106,162-164 (1957) Microscopic Theory of Superconductivity

[7] Cyrot .M. , D. Pavuna , Introduction to Superconductivity and High-Tc Materials, (1992)

[8] B. Josephson Phys. Lett. 1, 251 (1962)

[9] Thomas P. Sheahen, Introduction to High-Temperature Superconductivity

[10] Bednorz, J.G., Muller ,K.A. Possible High Tc Superconductivity in the Ba-La-Cu-O System, Z.Phys, **64** (1986) 189-193

[11] Jorgerson, J.D.,Schutterler ,H.B.,Hinks,D.G., Capone, D.W.,Lattice Instability and High –Tc Superconductivity in $La_{2-x}Ba_xCuO_4$, Phys. Rev. Lett. **58,10** (1987) 1024-1027

[12] Cava, R.J.,Van Dover , R.B., Battlog, B.,Rietman, E.A., Phys. Rev. Lett., **58,4** (1987) 408- 410

[13] Wu, M.K., Ashburn, J.R., Torng, C, Phys. Rev.Lett. **58,9** (1987) 908-910

[14] Kikuchi, M., Syono ,Y.,Tokiwa, A., Oh-Ishi, K., Arai, H., Hiraga, K.,Kobayashi, N., Sasaoka, T. and Muto, Y. , Jpn. Appl.Phys., **26, 6** (1987) L1066-L1069

[15] Michel , C., et al .,Z. Phys.B, Condensed Matter **68**, (1987) 421-423

[16] Maeda, H., Tanaka, Y., Jpn.Appl.Phys., **27,2** (1988) L209-L211.

[17] Tokano K. Appl. Phys.Lett. ,**53-14** (1988) 1329-1331

[18] Quidwai ,Ansar A, et al., Supercon.Sci.Technol.,**5** ,(1992) 602-604

[19] S. S. P. Parkin, V. Y. Lee, A. I. Nazzal, R. Savoy, T. C. Huang, G. Gorman and R. Beyers, Phys.Rev.B **38,** 6531 (1988).

[20] Z. Z. Sheng and A. M. Hermann, Nature **332**, 138 (1988).

[21] Nagamatsu , J., Nakagawa ,N., Muranaka, T., Zenitani ,Y., Akimitsu , J., Nature **410** (2001) 63-64

[22] A.C Rose-Innes and E.H. Rhoderic, Introduction to Superconductivity , Butterworth –Heineman, (1978)

[23] Arcroft , N.W., Mermin, N.D., Solid State Physics , Holt Rinehart & Winston (1976) .

[24] Oak. Ridge National Laboratory: Philip W .Philips

[25] Tokumitu, A., Miyake, K., Yamada, K., Crossover between Cooper-Pair Condensation and Bose-Einstein Condensation of "Di-Electronic Molecules" in Two-Dimensional Superconductors, Department of Physics, Nagoya University, Nagoya 63-73 , 464-01 (July 18, 1991)

[26] E. Maxwell, *Phys. Rev.* **78**, 477 (1950).

[27] Seeber, B., Handbook Of Apllied Superonductivity , (1998) , Universite de Geneve

[28] R.P. Huebener, *Magnetic Flux Structures in Superconductors*, edited by P. Fulde (Springer, Berlin, 1992).

[29] Vidali, G., Superconductivity: The Next Revolution? (Cambridge University Press, Cambridge [England]; New York, NY, USA, 1993).

[30] D. J. Bishop et al., Scientific American, 48 (Feb. 1993)

[31] Tinkham, M., *Introduction to Superconductivity* (McGraw-Hill, New York: 1975).

[32] M. N. Wilson, *Superconducting Magnets* (Oxford Univ. Press, New York: 1983).

[33] L. Goodrich and S. L. Bray, *Cryogenics* **30**, 667 (1990).

[34]. M.K. Wu, J.R. Ashburn, C. J. Torng, P.H. Hor, R.L. Meng , L.Gao,Z.J. Huang ,Y.Q. Wang, and C.W. Chu, Superconductivity at 93 K in a New –Mixed –Phase Y-B-Cu –O Compound Sytstem at Ambient Pressure , Phys. Rev. Lett. 58, 908- 910 (1987)

[35] S. Kambe ,Y.C Guo, S.X. Dou, H.K. Liu Proc. R. Soc. London **96** (1996) 454

[36] H. Maeda, Y.Tanaka, M. Fuktomi, T.Asano, Jpn.J. Appl. Phys., Part 2 **27** (1988) L 209

[37] H.L.Luo and Yu Mei, Thin Films of the High-T_c Bi-Sr-Ca-Cu Oxide System – A Brief Review,Chmin.J of Phys. **28**, No.5 (1990)